

**Reduction in shot blasting time for the vehicle
components of CNH prior to the coating
application and measurement of residual stress of
the blasted surface**

M. Tech Thesis

By

**Thakkar Dhruvil B.
(2202103013)**



**DEPARTMENT OF MECHANICAL ENGINEERING
INDIAN INSTITUTE OF TECHNOLOGY INDORE**

June 2024

Reduction in shot blasting time for the vehicle components of CNH prior to the coating application and measurement of residual stress of the blasted surface

A THESIS

Submitted in partial fulfillment of the requirements for the award of the degree

of

Master of Technology

by

THAKKAR DHRUVIL B.



**DEPARTMENT OF MECHANICAL ENGINEERING
INDIAN INSTITUTE OF TECHNOLOGY INDORE**

June 2024



INDIAN INSTITUTE OF TECHNOLOGY INDORE

CANDIDATE'S DECLARATION

I hereby certify that the work which is being presented in the thesis entitled **Reduction in shot blasting time for the vehicle components of CNH prior to the coating application and measurement of the residual stress of the blasted surface** in the partial fulfillment of the requirements for the award of the degree of **MASTER OF TECHNOLOGY** and submitted in the **DEPARTMENT OF MECHANICAL ENGINEERING, Indian Institute of Technology Indore**, is an authentic record of my own work carried out during the time period from July 2022 to June 2024 under the supervision Dr. Kazi Sabiruddin, Professor, Department of Mechanical Engineering.

The matter presented in this thesis has not been submitted by me for the award of any other degree of this or any other institute.

10/06/2024

**Signature of the student with date
Thakkar Dhruvil B.**

This is to certify that the above statement made by the candidate is correct to the best of our knowledge.

11/6/24

Signature of the Supervisor of
M. Tech. thesis (with date)

Prof. Kazi Sabiruddin

Thakkar Dhruvil B. has successfully given his M. Tech. Oral Examination held on **3rd June 2024.**

Signature of Supervisor of
M. Tech thesis

Date: 11/6/24

Convener

DPGC

Date: 11-06-2024

ACKNOWLEDGEMENTS

I extend my heartfelt appreciation to **CNH Industrial, Pithampur**, for funding the project and offering me access to their blasting facility. The opportunity to utilize the airless centrifugal blasting facility (i.e. wheel blast) has not only enhanced the quality of my research but has also allowed me to gather precise and reliable data crucial for the success of this project. I am sincerely grateful to the production team of Paint Shop 2 for their kind support and help during the experimental work conducted at CNH. I would also like to express my deepest gratitude and appreciation to my supervisor, **Prof. Kazi Sabiruddin**, of the Department of Mechanical Engineering, Indian Institute of Technology Indore, for his invaluable guidance, support, patience, and mentorship throughout my project work. I sincerely thank him for granting me the opportunity to work under his guidance.

My sincere thanks to **Dr. Abhijit Ghosh, Dr. Shahid Hussain, Mr. Setu Suman, Mr. Hitesh Patil, and Mr. Mahesh Malviy** for their continuous support and help throughout the project.

The people with the greatest indirect contribution to this work are **my parents**, who have been with me constantly and encouraged me throughout this work and in life as well.

Without their support, this thesis would not have been possible.

With Regards

Thakkar Dhruvil B.

**Dedicated to
my loving and caring parents.**

ABSTRACT

In the present study, different blasting parameters are varied to examine their roles on the quality of the steel (IS 2062) surfaces. The aim of this project work is to reduce the blasting time from 7 min to achieve SA 2.5 surface by selecting suitable process condition. Experiments are conducted on two blasting machines, namely the Suction-Type Blasting machine at IIT Indore and the Airless Centrifugal Blasting (Wheel Blast) facility of CNH Industrial (Paint Shop -2), Pithampur. The process parameters such as the material, size, and shape of blasting medium (shot/grit); and the blasting time are varied during the blasting operation. Steel shot, steel grit and alumina grit materials are employed in this study. Three different sizes of each material are selected for the blasting operations. Several blasting time durations are chosen to analyze the average surface roughness (Ra) and the quality of the produced surfaces. The surface roughness is measured by using contact type stylus profilometer. It is noticed that for each blasting condition, initially with increasing blasting time up to a certain duration the Ra value and the quality of the surface are increased. After reaching the maximum value the Ra tends to decrease with further increase in time. This is due to the over-blasting effect when the surface asperities are destroyed. Although with further increase in time Ra may increase again but it can never reach to the maximum due to the strain hardening effects. Hence, it is important and beneficial to consider the time when the Ra reaches the maximum. Among different blasting media alumina grits are found to produce the desired surface in rapid and effective manner. However, such medium can cause erosion to the wheel blades and embed on the produced steel surface as well. Steel grits are found to be more effective than steel shots in terms of removing the surface contaminants. Both the steel-based media (shot/grit) are safe for wheel blade as well as produced substrate surface. Larger shot/grit can produce the desired surface much faster than the smaller one. Due to the low accessibility to incoming shots the front, back, top, and bottom surfaces of any component do not get the desired surface even at the optimum blasting condition. By increasing the flow rate of shots, applying reflector plates at suitable locations, and orienting the rotors (wheels) in proper direction such problem can be avoided up to a certain extent. Further, the measurement of residual stress of the blasted surface is conducted using the X-Ray Diffraction method for different IS-2062 steel samples in both bare and blasted form. The samples are blasted with smallest and largest size of the steel shots, steel grits, and alumina grits that have been considered for this study. Also, the weight measurement of IS-2062 samples in different blasting conditions and different types of blasting media is done for a comparative study.

Contents

LIST OF FIGURES.....	ix
LIST OF TABLES	x
CHAPTER 1: Introduction.....	1
1.1 Surface Engineering	1
1.2 Surface Blasting on metallic surfaces	2
1.3 Blasting media and its types	2
1.4 About Case New Holland (CNH), Pithampur	4
1.5 Current Blasting conditions at CNH Pithampur.....	5
1.6 Literature review.....	6
1.7 Identified research gap and Objective of the project	7
1.8 Work Plan.....	8
CHAPTER 2: Experimental Procedure.....	9
2.1 Experimental Setup at IIT Indore and CNH Pithampur	9
2.2 Materials and Methods	9
2.3 Experiments performed at IIT Indore.....	12
2.4 Experiment performed at CNH Pithampur	12
2.5 Measurement of Residual Stress using X-Ray Diffraction (XRD) method.....	15
2.6 Microhardness Analysis	16
CHAPTER 3: Results and Discussion.....	17
3.1 Average surface roughness (Ra) analysis of IS 2062 when blasted with steel shots	17

3.2 Average surface roughness (Ra) analysis of IS 2062 when blasted with various blasting media	22
3.3 Comparison of various blasting media w.r.t. blasting time	28
3.5 Outcomes from the experiments at CNH Pithampur	31
3.6 Results of the residual stress analysis.....	32
3.7 Observations from the Vickers Microhardness analysis of the cross section of the blasted samples	40
3.8 Weight measurement of IS-2062 steel samples and different blasting media	43
CHAPTER 4: Conclusion	48
REFERENCES	51

LIST OF FIGURES

Figure 1. Aluminum Oxide grits[5]	3
Figure 2. Glass Beads[6]	3
Figure 3. Steel Shots[7]	4
Figure 4. Work Plan	8
Figure 5. Centrifugal Blasting facility at CNH Pithampur	9
Figure 6. Suction type blasting facility at IIT Indore	10
Figure 7. Welded steel samples cut in specific dimensions suitable for the experiments	11
Figure 8(a) and (b). Sample attached to the holder frame and Six holder frames hung from the conveyor shaft with the help of S-hooks	13
Figure 9. Schematic diagram of experimental setup at CNH	13
Figure 10. SA 2.5 Surface Quality tester	14
Figure 11. Stylus Profilometer	15
Figure 12. Schematic diagram of sample arrangement related to phi-psi method for XRD Analysis	15
Figure 13. Plots of Ra v/s Time related to Steel Shots	19
Figure 14. Comparison of different shots (size) to achieve the maximum Ra	21
Figure 15. Ra v/s time for Alumina grits, Steel Shots and Steel Grits of 16 mesh	24
Figure 16. Ra v/s time for Alumina grits, Steel Shots and Steel Grits of 18 mesh	26
Figure 17. Ra v/s time for Alumina grits, Steel Shots and Steel Grits of 20 mesh	27
Figure 18. Normal XRD scan of the blasted sample at CNH Pithampur	33
Figure 19. Residual stress analysis of the sample blasted at CNH Pithampur	34
Figure 20. Gauss fit to calculate the peak position of XRD analysis for un-blasted sample	35
Figure 21. Schematic diagram of the types and directions of stresses induced due to application of load on a specimen	37
Figure 22. Comparison of residual stress among the samples blasted with different blasting media and mesh sizes	40
Figure 23. Vickers microhardness data plot for Alumina grits 16 mesh size and 20 mesh size	41
Figure 24. Vickers microhardness data plot for Steel grits 16 mesh size and 20 mesh size.	42
Figure 25. Vickers microhardness data plot for Steel shots 16 mesh size and 20 mesh size	42
Figure 26. Weight Loss of IS-2062 samples when blasted with steel grits	44
Figure 27. Weight loss of IS-2062 samples when blasted with Alumina grits	44
Figure 28. Weight loss of IS-2062 samples when blasted with Steel shots	45
Figure 29. Comparison of Single impact weight for various blasting media	46

LIST OF TABLES

Table 1.Current blasting conditions at CNH Pithampur	6
Table 2.Cast analysis for IS-2062 steel (as received from CNH)	11
Table 3.Process variables for blasting by suction type blasting at IIT Indore.....	12
Table 4.Results regarding steel shots as blasting media	22
Table 5.Comparison of different blasting media w.r.t. blasting time	29
Table 6.Overall comparison of blasting media.....	30
Table 7.Variation of Ra with varying blasting time for different surfaces of a component prepared by the Wheel Blast System of Paint Shop 2, CNH Pithampur	32
Table 8.d-spacing using Bragg's Law for blasted sample at CNH	36
Table 9.d-spacing using Bragg's Law for un-blasted sample	36
Table 10.Calculation of laboratory strain values for the sample blasted at CNH	37
Table 11. Comparison of depth of residual stress generated on IS-2062 when blasted with different blasting media and size	43

CHAPTER 1: Introduction

1.1 Surface Engineering

Surface engineering is the science that deals with improving the properties of the material surface so that apart from enhancing the life of the component, other properties for a specific requirement can be imparted. Improving the surface properties becomes the primary solution when mostly the failure begins from the surface because of poor mechanical properties, irregularities, and defects.

Surface engineering by application of various types of coatings is described as the process of establishing a surface that has features that differ from the bulk material in terms of improving the engineering product's life and functionality. The desired properties or characteristics of surface-engineered components include:

Abrasion wear resistance, improving aesthetic look, improving mechanical, electrical, and optical properties, and increasing the surface finish

Surface roughness is a vital factor in surface engineering, affecting the tribological properties like wear resistance and frictional behavior of metallic parts.

Various parameters, such as average roughness (Ra), root mean square roughness (Rq), and peak-to-valley height (Rz), are typically used to characterize surface roughness. These metrics quantify surface texture and are essential for understanding how a surface will interact with other materials or coatings. In surface engineering, controlling, and optimizing surface roughness is crucial to improving the performance and durability of components under various wear conditions, including adhesive, abrasive, and erosive wear[1].

1.2 Surface Blasting on metallic surfaces

Blasting is a widely used industrial process aimed at altering the surface characteristics of metallic materials. This method entails the high-speed application of abrasive particles onto the surface, effectively eliminating contaminants, rust, and old coatings. Additionally, it helps attain a predetermined degree of surface roughness.

Blasting with different abrasive materials, such as steel grit and alumina, effectively increases surface roughness. This increased roughness can improve the adhesion strength of coatings and enhance corrosion resistance. However, the choice of abrasive material and blasting parameters significantly affect the resultant surface properties [2].

1.3 Blasting media and its types

Blasting media are materials used in abrasive blasting processes to clean, roughen, or polish surfaces by propelling particles at high speeds. These materials vary widely in terms of their composition, size, and hardness, each offering specific advantages for different applications.

The choice of blasting media is critical to the success of the blasting process, influencing factors such as surface cleanliness, texture, and preparation for subsequent coatings or treatments. Each type of media is suited to specific tasks and substrates, ensuring the efficiency and effectiveness of the blasting operation while minimizing environmental impact and health risks associated with dust and residues.[3]

The different types of blasting media can be listed as follows[4]:

- 1. Aluminum Oxide:** This media is widely used due to its hardness and durability. It is effective for removing rust, paint, and coatings from various surfaces. Aluminum oxide is also known for its ability to create a uniform surface texture, making it suitable for preparing surfaces for further treatment, such as painting or coating.



Figure 1. Aluminum Oxide grits[5]

- 2. Glass Beads:** Glass beads are used for cleaning and finishing surfaces. They provide a smooth, bright finish without significantly removing material from the substrate. This makes them ideal for applications where minimal abrasion is required, such as cleaning delicate parts or polishing metal surfaces.



Figure 2. Glass Beads[6]

- 3. Steel Grit and Steel Shot:** These media are preferred for heavy-duty cleaning and surface preparation. Steel grit, with its angular shape, is effective for removing coatings, rust, and other contaminants, while steel shot, with its spherical shape, is used for peening and polishing metal surfaces. Both media types are known for their high impact energy, which enhances the cleaning and surface preparation process



Figure 3. Steel Shots[7]

- 4. Plastic Media:** Plastic media are used for more delicate applications where less aggressive abrasion is required. They are commonly used in the aerospace and automotive industries for stripping paint and coatings without damaging the underlying substrate. Plastic media are also effective for deburring and de-flashing molded plastic parts.
- 5. Organic Media:** Materials such as corn cobs and walnut shells are environmentally friendly options used for blasting. These media are ideal for softer cleaning surfaces, such as wood and plastics, without causing damage. Organic media are also used in applications where the removal of residues and contaminants is required without the introduction of harmful substances.

1.4 About Case New Holland (CNH), Pithampur

The CNH plant located in Pithampur, Madhya Pradesh, India, produces a wide range of products including loader backhoes, compactors, and crawler excavators. The facility services the Indian domestic market and exports to more than 75 countries in Africa, the Middle East, the Asia Pacific region North and Latin America.

The factory was built in 1989, and in 2022 celebrated the significant milestone of 50,000 loader backhoes produced. Today, the manufacturing complex is spread over an area of 40 acres. It is aligned with the Indian government's initiatives such as Make-in-India and Aatmanirbhar Bharat, with its compactor and loader backhoe production being more than 90%

localized. Its production activity is supported by an advanced Research & Development Center, and in 2022 it inaugurated a new Operator Training Center. The facility operates with a strong focus on sustainability. Its environmental initiatives include the installation of solar panels, which provide up to 25% of its energy, as well as recycling and re-using practices that have significantly reduced its waste materials and water consumption. It achieves consistently high quality with its class-leading and automated production technologies, which include robotic welding, laser cutting and high-precision machining. It has ISO certifications for its Quality, Health & Safety, Environmental and Energy performance. [8]

1.5 Current Blasting conditions at CNH Pithampur

The plant houses a powder coating paint shop which has an airless centrifugal blasting facility (also known as Wheel Blast) for the cleaning and preparation of parts prior to the coating applications. A suitable surface quality and roughness is desired on the parts for strong coating-substrate adhesion through mechanical anchorage. This facility uses the continuous movement of parts using roller conveyors through the blasting chambers with a selected speed so that the desired surface roughness (Ra) of around 6 to 8 μm and the desired surface quality of SA 2.5, is obtained for all the components irrespective of their size, shape, etc. Currently, the time taken by a single trolley (the entity on which the parts to be blasted are hung on the overhead conveyor) to pass through the blasting chamber and get the desired surface quality and roughness for all the components is around 7 minutes. The details of the blasting conditions currently followed by Paint Shop 2 of CNH are depicted in Table below:

Table 1. Current blasting conditions at CNH Pithampur

Blasting Technology	Airless Centrifugal Blast Blade (<i>Disha India</i>)
Length of Blasting Chamber	5.53 m
Conveyor Speed (by changing frequency parameter in Hz)	0.8 m/min
Blasting time (each trolley)	6.9 min
Workpiece Material	IS 2062 Steel
Workpiece/Trolley Size (max.)	3.7 x 2.3 x 1.7 m ³
Blasting Medium	Hardened Steel Shots
Shape of Blasting Medium	Spherical
Shot Size	S-330 (841 μm)
Application of Reflector Plates for bottom surface	Yes

1.6 Literature review

- Bahbou et al. (2004) noticed that the maximum coating adhesion was observed post blasting at 90° impingement angle to create the surface roughness for the coating application.[9]
- James Day et al. (2005) concluded that to improve the bond strength, the blasting pressure, the number of passes and grit size should be increased.[10]
- K Poorna Chander et al. (2009) studied that grit blasted surface possesses compressive residual stress which increases with both blasting pressure and blasting angle. There is an almost linear correlation between the Barkhausen noise signal, and the measured compressive residual stress of grit blasted low carbon steel surfaces.[11]
- M Multigner et al. (2009) studied grit blasted Ti6-Al-4V alloy. It was concluded that there is severe plastic deformation of the surface. The

hardening effects were not significant at the sub-surface zone, which indicates the low hardening co-efficient of the alloy. [12]

- Vishal Sharma and Kazi Sabiruddin (2020) carried out a comparison study of sand blasted and EDM-ed surfaces of steel substrates. They have concluded that the sand blasted surface contains a uniform strain hardened zone. The hardening effect increases with an increase in kinetic energy of grits. EDM-ed surface does not adhere to the coatings.[13]
- Prathamesh Tawade et al. (2023) studied the effects of different environments related to grit blasting on the prepared steel surface. The study related to the average surface roughness (Ra) showed that Highest Ra on mild steel in dry conditions was obtained by using 16 mesh size Alumina grits, 80mm Stand Off Distance and 45 seconds of blasting time.[14]
- M. Praveen et al. (2023) carried out the surface cleaning of IS-2062 E350 grade steel plates using a multi table air type shot blasting machine. It was observed that 50 μ m surface roughness was obtained with a blasting time of 12 minutes using the above method.[15]

1.7 Identified research gap and Objective of the project

Based on the review of the past work done research gap is identified. To the best of our knowledge, few literature has been found on grit blasting and its applications, but no one has studied regarding the blasting parameters of airless centrifugal blasting machine (also known as Wheel Blast). Also, very few literature related to blasting operation on IS-2062 industrial grade steel, as a substrate has been noticed till date. The aim of this project is to reduce the blasting time of components blasted with Wheel blast facility, such that the desired surface quality and roughness are obtained within the stipulated blasting time. The other objective of the project is to measure the residual stress developed in IS-2062 steel because of blasting operation on the surface and perform weight measurement analysis for IS-2062 substrate and different blasting media w.r.t different blasting conditions.

1.8 Work Plan

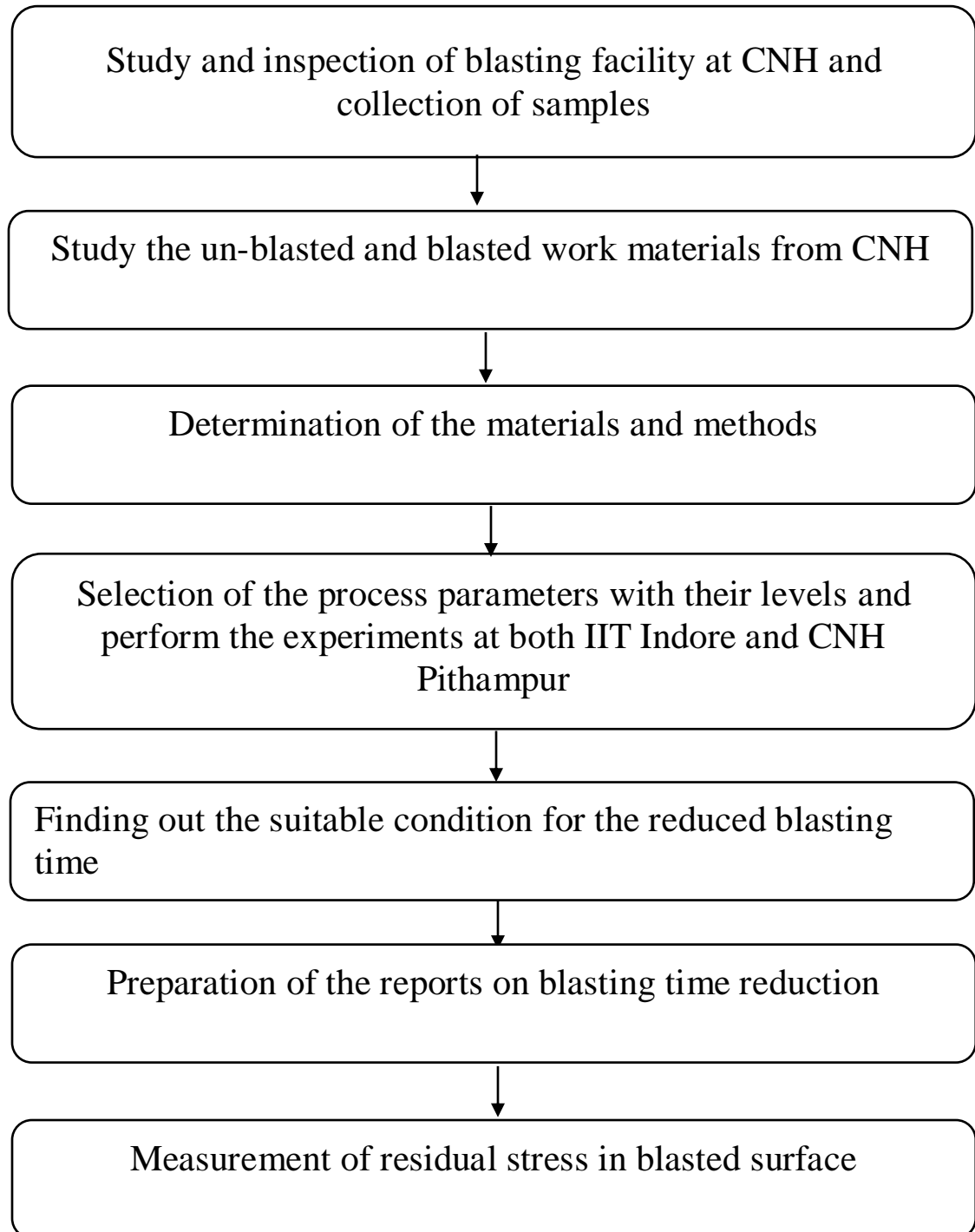


Figure 4. Work Plan

CHAPTER 2: Experimental Procedure

2.1 Experimental Setup at IIT Indore and CNH Pithampur

The experiments related to the project were conducted at both IIT Indore and CNH Pithampur. To avoid any work hindrance and to maintain the regular productivity of the plant a major part of the project work is conducted at IIT Indore, and one experiment is conducted at CNH Pithampur. The experiments related to blasting media are conducted at the Suction Type blast cabinet available at IIT Indore. Hence the quantitative data obtained from such experiments with Suction Type blasting facility may differ from the same of the Wheel blast. However, the qualitative comparison among different blast media in terms of their material, shape and size remains the same for both the blasting systems.

2.2 Materials and Methods

Figure 5 shows the actual and schematic photographs of the Airless Centrifugal Blast/Wheel Blast (Disha India) facility installed at the Paint Shop-2 of CNH Pithampur. It contains a total of 16 rotors in two adjacent chambers with 8 rotors in one. The 8 rotors are mounted on the two side walls (4+4) of a chamber. When the components carried by an overhead

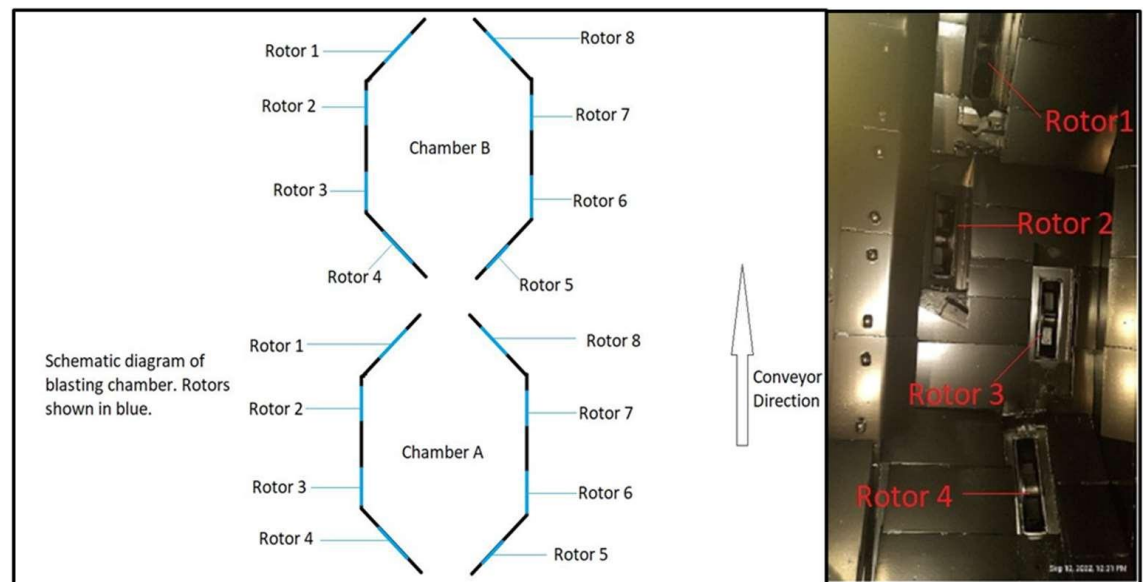


Figure 5. Centrifugal Blasting facility at CNH Pithampur

conveyor move from one chamber to another the rotors start operating in a sequential manner.

The blasting facility at IIT Indore comprises of Suction type blasting cabinet (Synco Industries' SSB-606060) shown in Figure 2. This facility works with the help of the suction of blasting media into the hose pipe arrangement of the machine. The compressor is arranged along with the machine so that the pure and compressed air is useful for the suction of the blasting media to impinge the particles on the workpiece at high velocity. The workpiece is placed in the blasting chamber by maintaining a suitable SOD from the blasting nozzle. The blasting is carried out continuously for the required time while the time is recorded manually by using a stopwatch. The SOD of nozzle while blasting is kept 50mm, and the blasting pressure is equal to 5bar.



Figure 6. Suction type blasting facility at IIT Indore

Such a blasting facility works with relatively lower pressure, flow rate, speed, and SOD than that of Wheel Blast facility at CNH. Hence, the produced average surface roughness (Ra) by this equipment will be lower than the same of Wheel Blast type equipment. However, the trend of Ra

from such equipment will be like the same produced by the Wheel Blast system.

The substrate (i.e. workpiece surface) material used for this study is IS-2062 steel as the same is used to produce the components. The composition (%) of IS-2062 steel (as received from CNH) is shown in Table 2.

Table 2. Cast analysis for IS-2062 steel (as received from CNH)

Element	C	Mn	S	P	Si	Al	Cr	Cu	Ni	Ti	V	Nb	Mo	N
Content (%)	0.153	1.241	0.0022	0.014	0.205	0.038	0.025	0.065	0.024	0.014	0.005	0.016	0.006	0.0044

The sample steel plates are collected from CNH and a few of those are blasted with the current blasting condition (as shown in table 1) for further studies at IIT Indore. A few weld beads are deposited randomly on the plates by using MAG welding facility to replicate actual surface condition prior to the blasting operations. These bare plates with welded beads, spatter, scales, and oxide layers are cut into 45 mm x 45 mm x 7 mm dimensions (Figure 7) for further experiments with Suction type blasting facility.



Figure 7. Welded steel samples cut in specific dimensions suitable for the experiments

The study of the blasted surface has revealed that the surface is of SA 2.5 quality with a Ra value of around 6 to 7 μm . This surface is considered as the standard for further studies.

2.3 Experiments performed at IIT Indore

The experiments on varying blasting media (material, shape, size) have been conducted at IIT Indore with the Suction type blasting facility. The effects of those media related parameters on the blasting time and surface quality are studied in detail. Table 3 shows the process variables and their levels used for conducting the experiments. The blasting operation is carried out for individual sample for each of the combination in the table listed below, to analyze the surface roughness in each case.

Table 3. Process variables for blasting by suction type blasting at IIT Indore

Variables	Level/Type
Blasting Media	Steel shot (spherical)
	Al ₂ O ₃ grit (irregular)
	Steel grits (irregular)
Size of Blasting Media (Mesh no. and microns)	16 (1190 μm)
	18 (1000 μm)
	20 (841 μm)
Blasting Time by Suction Cabinet (s)	5, 10, 15, 30, 45, 60, 75, 90, 105, 120, 135, 150, 165, 180

2.4 Experiment performed at CNH Pithampur

The effect of varying shot blasting time on the surface quality of IS 2062 steel plates is studied by using S-330 shots in the Wheel Blast system at CNH Pithampur. The blasting time is reduced from the current value (7 min) by increasing the conveyor speed through increasing the frequency of the current to the conveyor motors, with the help of Siemens Micromaster 420 controller. The frequency of the current varied from 18.7 Hz to 42.7 Hz with

a step size of 6 Hz. The plate samples are temporarily fixed with the holder frame which is further hung from the conveyor trolley shaft. For each frequency (i.e. blasting time) six samples are hung to represent the six different surfaces of a rectangular cuboid as shown in Figure 8 (a and b) and Figure 9. This experiment is conducted to see the effect of blasting time on the top, bottom, front, rear, lefthand side and righthand side of a three-dimensional component.



Figure 9(a) and (b). Sample attached to the holder frame and Six holder frames hung from the conveyor shaft with the help of S-hooks

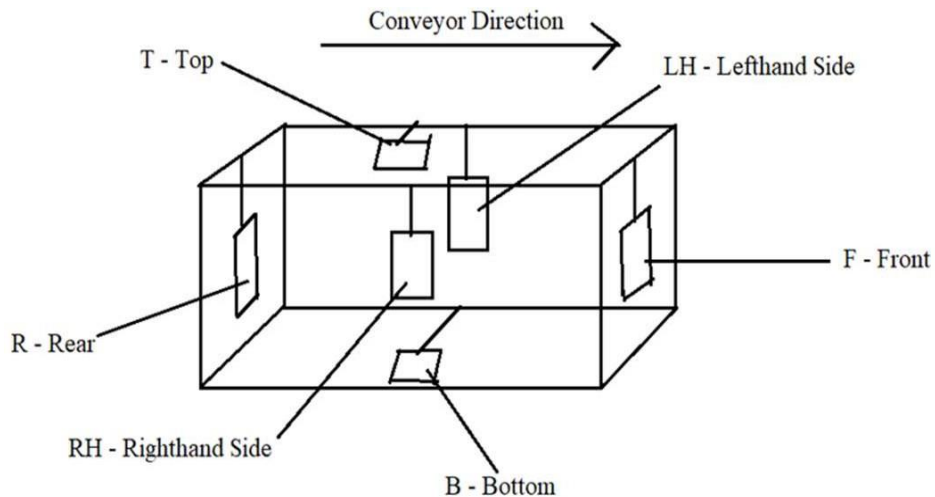


Figure 8. Schematic diagram of experimental setup at CNH

The shot blasting is carried out for each conveyor speed (i.e. blasting time) and following that, the blasted samples are checked for the SA 2.5 quality standard. This check is performed using the in- house facility provided by CNH Pithampur. Next, the surface roughness (Ra) measurement of the blasted samples is done at IIT Indore using the Stylus profilometer (Taylor Hobson Surtronic 25). The tip of the stylus contacts the surface asperities and moves along the traverse axis. The stylus sensor measures the different surface roughness parameters. The transducer connected opposite to the stylus is responsible for converting vertical movement into an electrical signal. The figures of both the devices are shown in Figure 10 and Figure 11 respectively.



Figure 10.SA 2.5 Surface Quality tester



Figure 11. Stylus Profilometer

2.5 Measurement of Residual Stress using X-Ray Diffraction (XRD) method

The measurement of residual stress for samples blasted with various blasting parameters is carried out using the phi-psi (Φ - Ψ) method using an Empyrean X-ray Diffractometer (Malvern PANalytical) equipped with Cu- $K\alpha$ radiation ($\lambda=1.54187\text{nm}$). The Φ - Ψ method determines stresses in different orientations relative to the material's surface. Phi (Φ) represents the azimuthal angle, which is the angle of rotation around the normal to the surface. Psi (ψ) denotes the tilt angle, which is the angle between the normal to the surface and the diffraction vector.

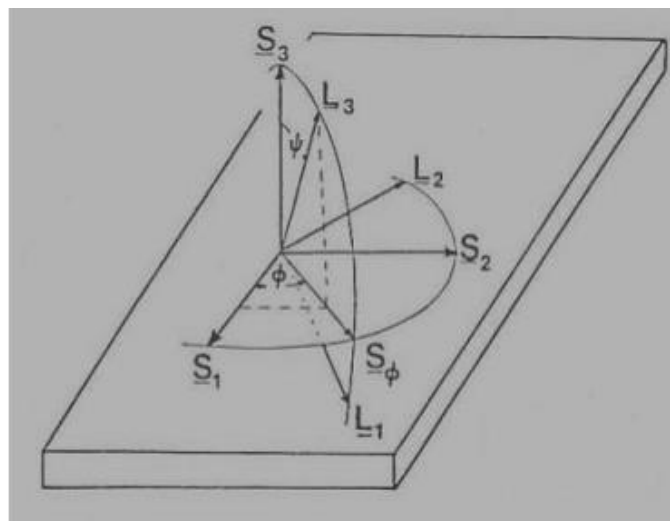


Figure 12. Schematic diagram of sample arrangement related to phi-psi method for XRD Analysis

In the above figure. Ψ is tilt angle Φ is rotation angle. S1, S2 and S3 are the axes of sample and L1, L2, L3 refer to laboratory system, i.e. the temporary axes of the sample when the sample is tilted for the scan with the respective parameters in an XRD setup.

XRD analysis is conducted for both bare condition (i.e. un-blasted sample received from CNH Pithampur) and blasted condition for IS-2062 samples to calculate the residual stress using the d-spacing comparison in each case. Initially a phase scan is carried out for the blasted sample (with current blasting conditions at CNH Pithampur) from 2θ angle 30° to 130° . The result of the phase scan was analyzed carefully and finally the peak which appeared around 2θ angle 82° (211 peak) was selected for residual stress analysis further in the experimental work. Further the scans were conducted from range 80° to 84° with the step size of 0.04° . These scans are performed with different combinations of phi-psi (Φ - Ψ) angles. The results are used to calculate the d-spacing and subsequently, the residual stress.

2.6 Microhardness Analysis

The hardness, which is the characteristic of the material, is defined as the resistance against indentation. It is measured by making a permanent indentation on the material and measuring its diagonals of the indent d_1, d_2 . The microhardness analysis is carried out for the IS-2062 samples blasted with the blasting media available in the highest and the lowest mesh size (i.e. 16 mesh size and 20 mesh size). The samples are cut, and the cross section of the respective sample is polished highly so that the impressions can be identified clearly to measure their diagonals. With the help of the microhardness analysis at the cross section of the blasted samples, the depth of the residual stress in the sample can be estimated. The Mitutoyo HM-220 microhardness tester is used for the analysis. The indentations are initially marked at the base of the cross section to calculate the average hardness of the base, keeping the dwell time 15 seconds and normal load of 50gf. Further, the indentations are marked at distance of $40\ \mu\text{m}$, $80\ \mu\text{m}$, $120\ \mu\text{m}$,

160 μm and 200 μm from the blasted surface to record the hardness of the cross section at each point, keeping the dwell time and the normal load same. Hardness is calculated using the standard formula:

$$\text{Vickers hardness} = 1.854(F/d^2) \quad [16]$$

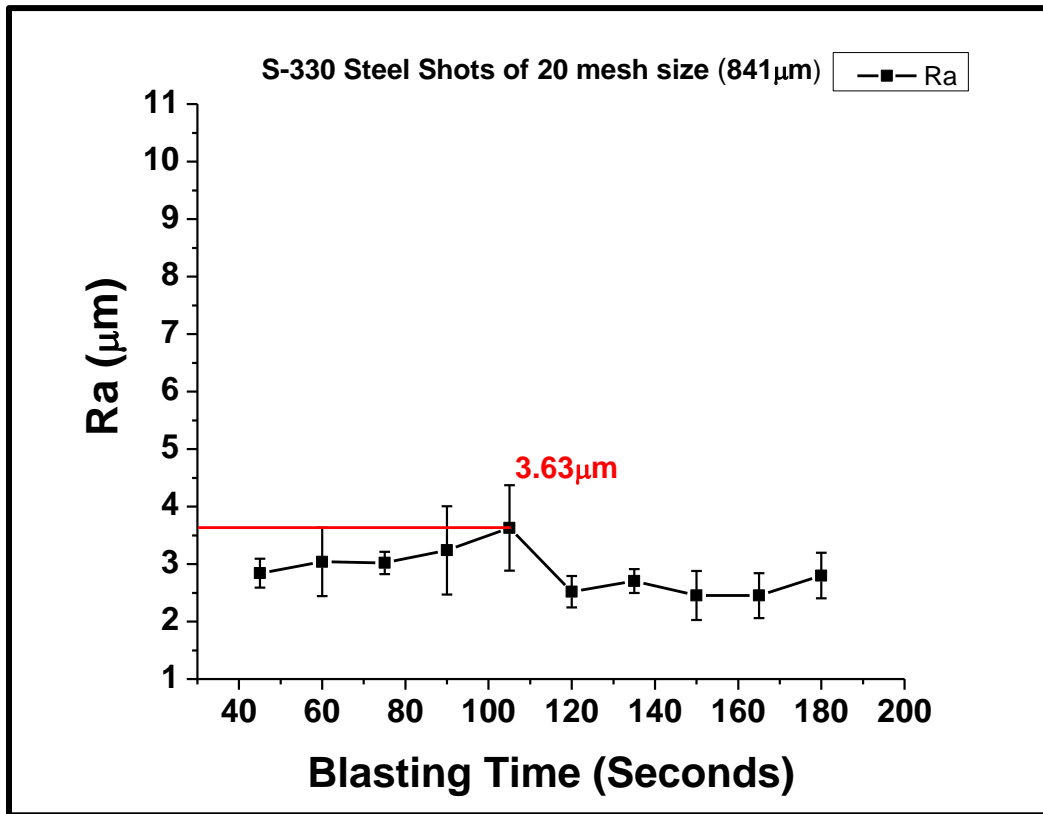
Here F = applied force in gf, d = average length of diagonals in microns (μm). This data is plotted as a graph of depth of cross section v/s micro-hardness value. The best fit line is fitted for the data plot obtained. This best-fit line is extrapolated up to the point where it meets the line of the base hardness, which is calculated earlier for the record. The distance up to the point where the extrapolated best fit line meets the base hardness can be considered the depth till which residual stress is present in the blasted sample.

CHAPTER 3: Results and Discussion

3.1 Average surface roughness (Ra) analysis of IS 2062 when blasted with steel shots

CNH currently uses hardened steel shots of 20 Mesh size for their airless centrifugal blasting facility. Hence, the experiments are started with the

hardened steel shots. The blasting operation was done from 45 seconds to 180 seconds with 15 seconds increment after each blasting operation. The variation of average surface roughness (Ra) with respect to blasting time for different steel shots is shown in Figure 13. In all the cases, the Ra value is initially increased with increasing blasting time and reached to the maximum. With further increase in blasting time, the Ra value tends to decrease and increase again. However, the Ra could never reach to the maximum value again due to the enhanced surface hardening effect by the long blasting time.



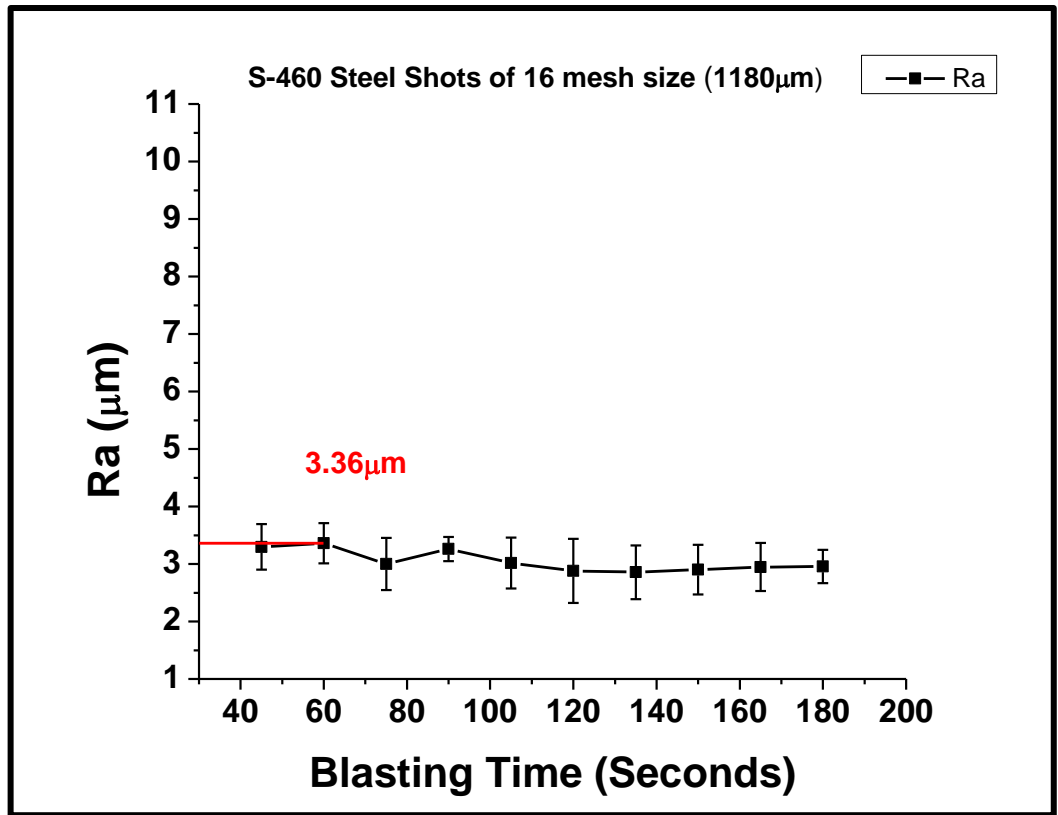
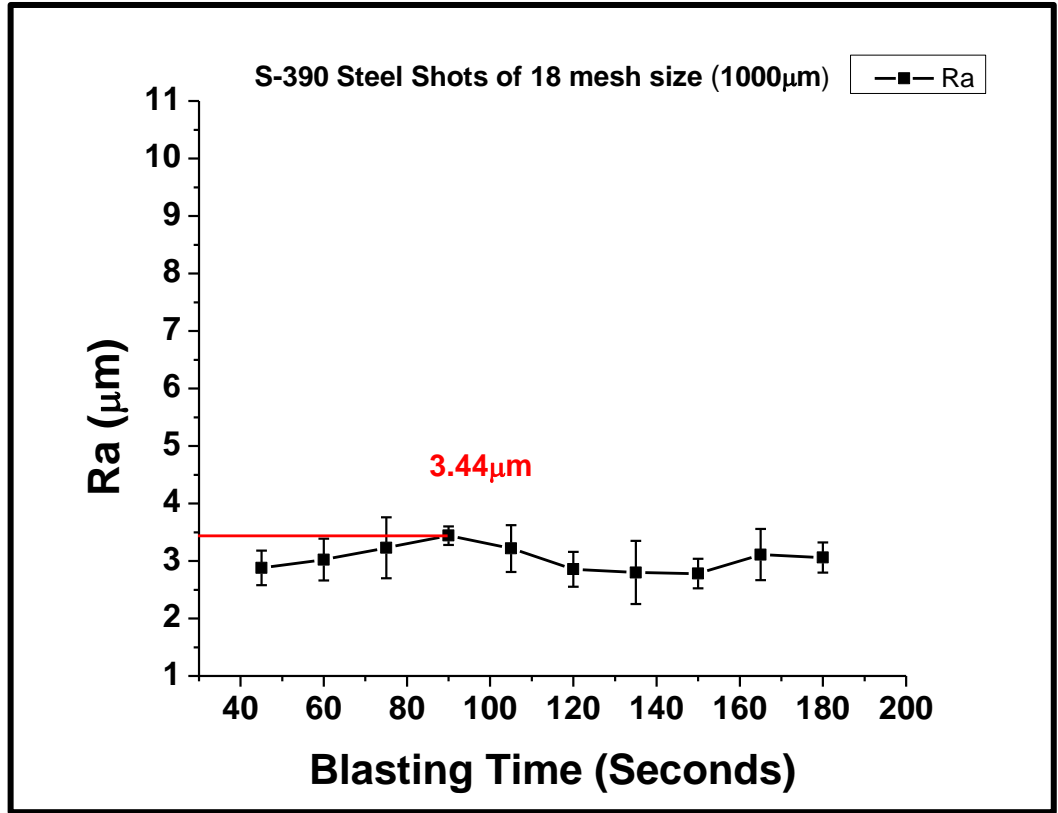


Figure 13. Plots of Ra v/s Time related to Steel Shots

From the plots, it can be observed that the time taken to reach the maximum Ra decreases significantly as the size of the steel shot is increased from 841 μm to 1180 μm . This reduction in time is observed because of the size of the deformations caused by the steel shots on the surface of the substrate. Larger-size deformations by larger steel shots take less time to generate surface roughness.

In this study, the time taken to reach the first peak of the plot of surface roughness is considered. This is because, as the bare samples are blasted initially, the blasting media creates irregularities on the surface of the substrate, causing the maximum initial peak of roughness. Further blasting beyond the first maximum peak leads to the sub-surface hardness by work hardening due to the impingement of blast media on the substrate surface. Now, if the blasting is continued further, these irregularities generated on the substrate are destroyed by the over-blasting of the substrate. The cycle will start again, and fresh irregularities will be created on the substrate's surface. Here in the further cycles, the roughness of the substrate surface does not reach or cross the value of the initial roughness observed. The reason for this is the sub-surface hardness created by the initial blasting of the substrate. Thus, the time taken to reach the first maximum/peak of the surface roughness value (Ra) by a particular blasting media is concerned. Irrespective of the blasting system a similar trend will be observed.

Comparing the blasting facility at CNH Pithampur, i.e. the airless centrifugal blasting facility/Wheel Blast system and that at IIT Indore, i.e. the suction type blasting facility it is observed that much higher maximum Ra value (above 6 μm) can be obtained from Wheel Blast system due to its capability of throwing the shots with a very high speed or kinetic energy. The maximum Ra value obtained by the suction-type blasting cabinet is around 3.5 μm because of its capacity limitations.

Figure 14 shows the comparison among the steel shots of different sizes based on blasting time to reach the maximum Ra value.

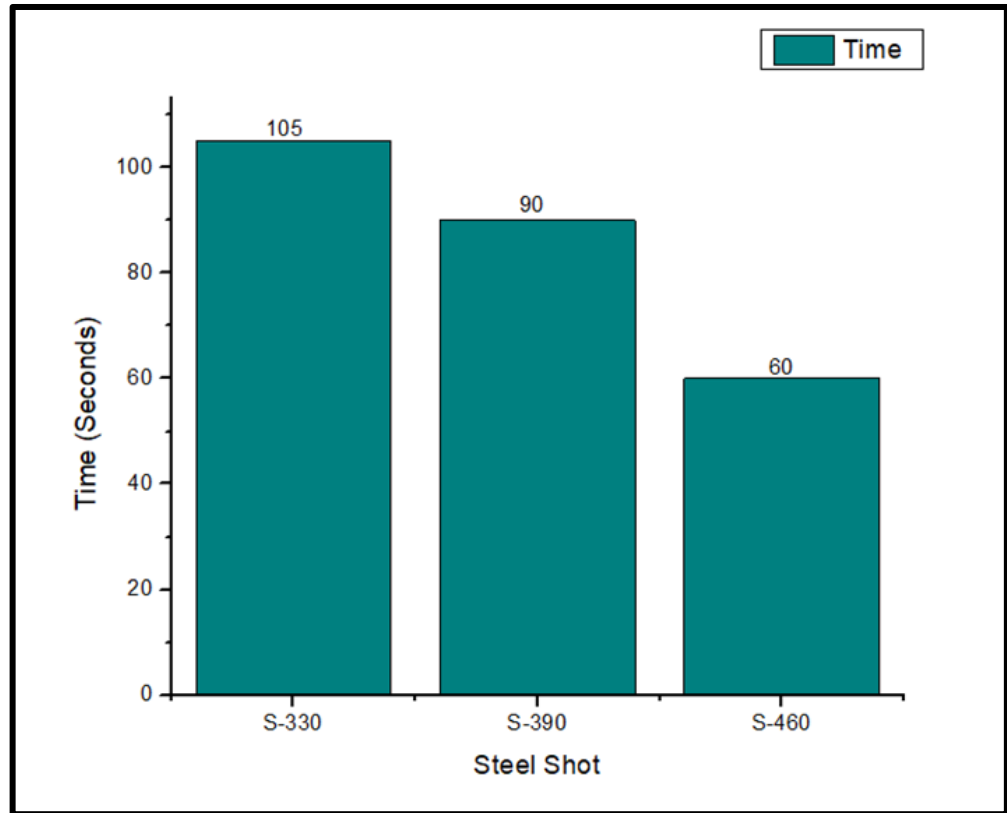


Figure 14. Comparison of different shots (size) to achieve the maximum Ra

In the above graph, S330 refers to steel shots of 20 Mesh size.

S390 refers to steel shots of 18 Mesh size.

S460 refers to steel shots of 16 Mesh size.

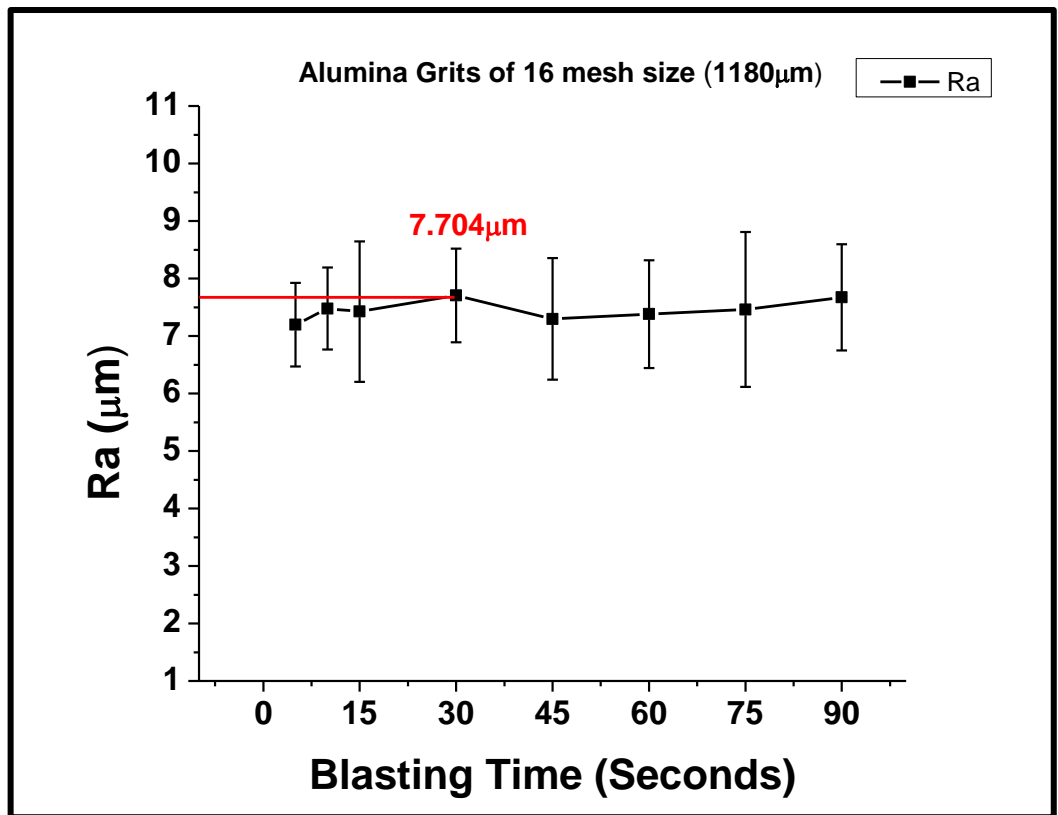
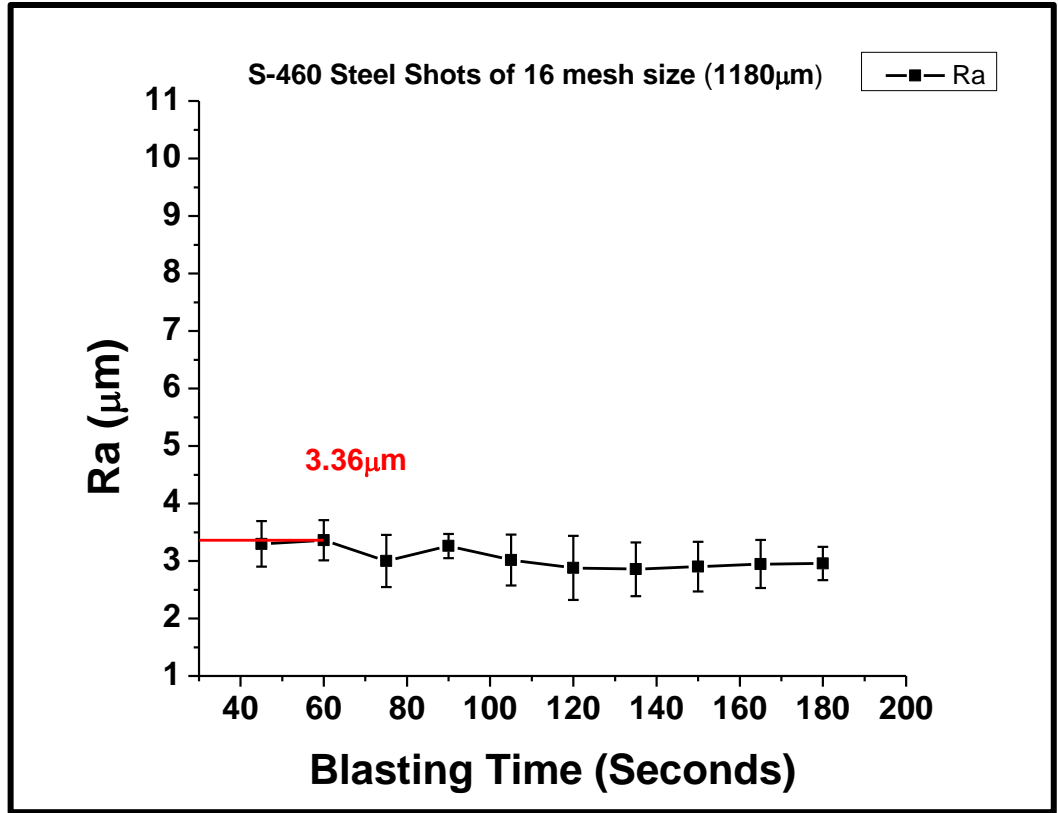
The overall comparison and results regarding the steel shots are mentioned in table 4. It can be observed from the table that; 60 to 180 seconds can be saved if S-390 or S-460 steel shots are employed in place of S-330 steel shots, respectively.

Table 4. Results regarding steel shots as blasting media

Blasting System	Shot Type	Maximum Ra (μm)	Time (s)	Remarks (Time Saved)
Suction Type (simulated)	S-330 (841 μm) Steel Shots (20mesh)	3.63	105	Default
	S-390 (1000 μm) Steel Shots (18 mesh)	3.44	90	Model 1: Comparison of S-330 and S-390 $((105-90)/105) \times 100 = 14.3\%$
	S-460 (1180 μm) Steel Shots (16 mesh)	3.36	60	Model 2: Comparison of S-330 and S-460 $((105-60)/105) \times 100 = 42.8\%$
Airless Centrifugal Type (actual)	S-330 Steel (841 μm) Shots (20 mesh)	7	420	<ul style="list-style-type: none"> • Using Model 1: $420 \times 0.143 = 60\text{s}$ Saved • Using Model 2: $420 \times 0.428 = 180\text{s}$ Saved

3.2 Average surface roughness (Ra) analysis of IS 2062 when blasted with various blasting media

The next set of experiments involved changing the material of the blasting media. The size of the blasting media is kept constant for effective comparison. Figures 15, 16 and 17 show the plots of Ra with varying blasting time. Clearly, in all the cases the maximum Ra is achieved after a specific time of blasting. However, the time and value of the maximum Ra for each blasting media is varied with varying blasting material.



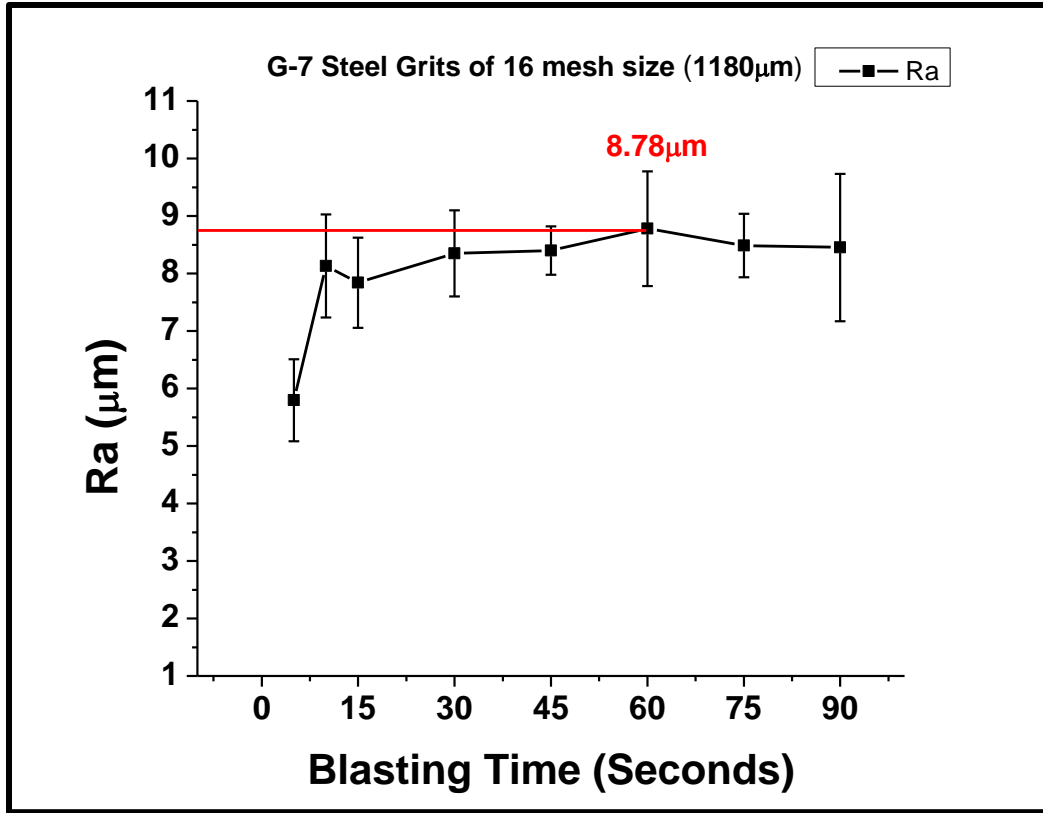
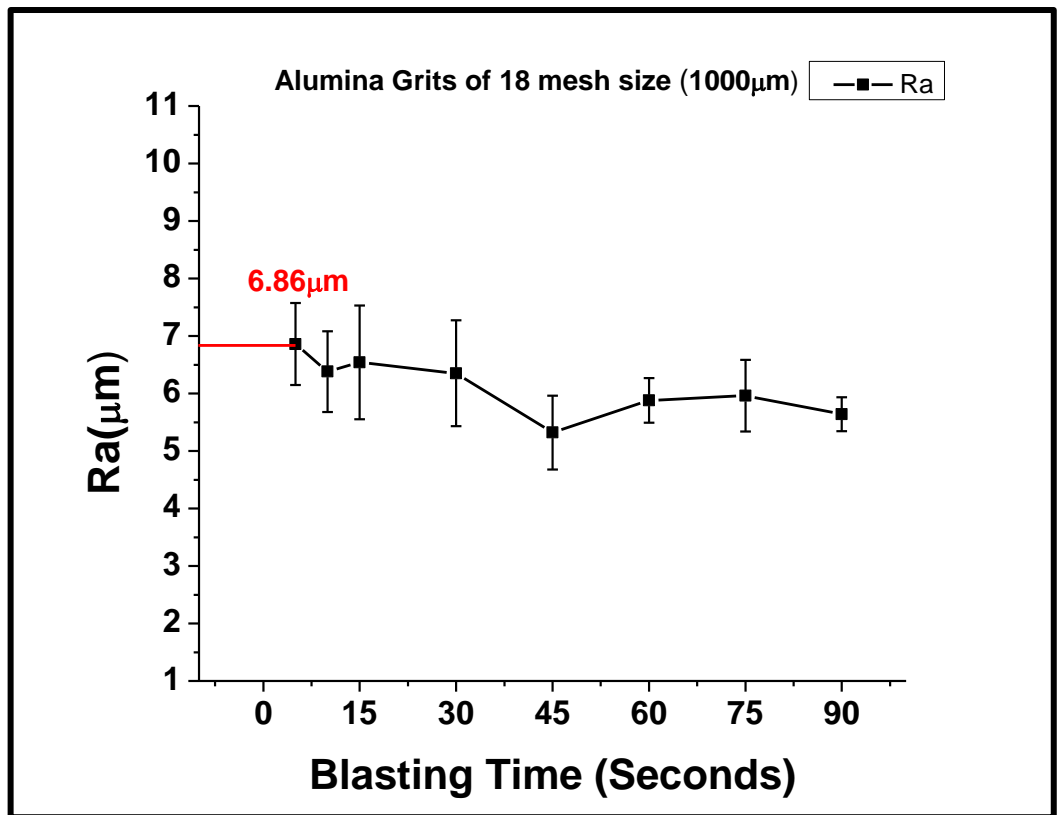
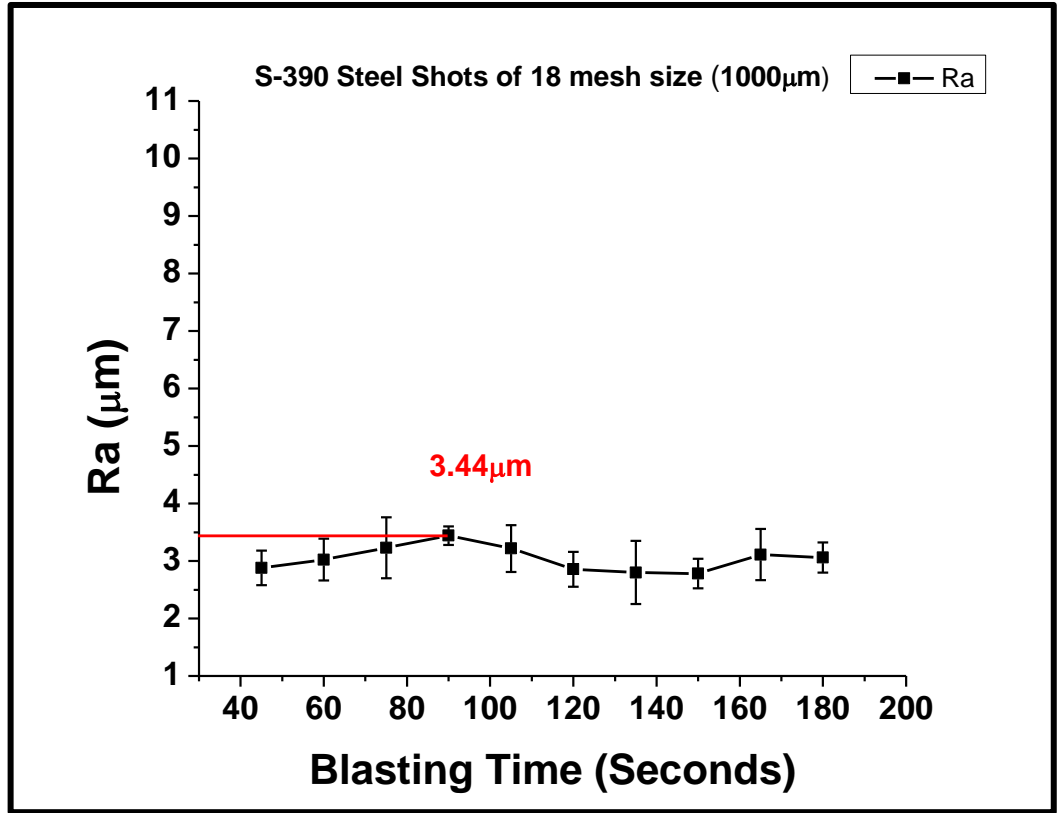


Figure 15. Ra v/s time for Alumina grits, Steel Shots and Steel Grits of 16 mesh



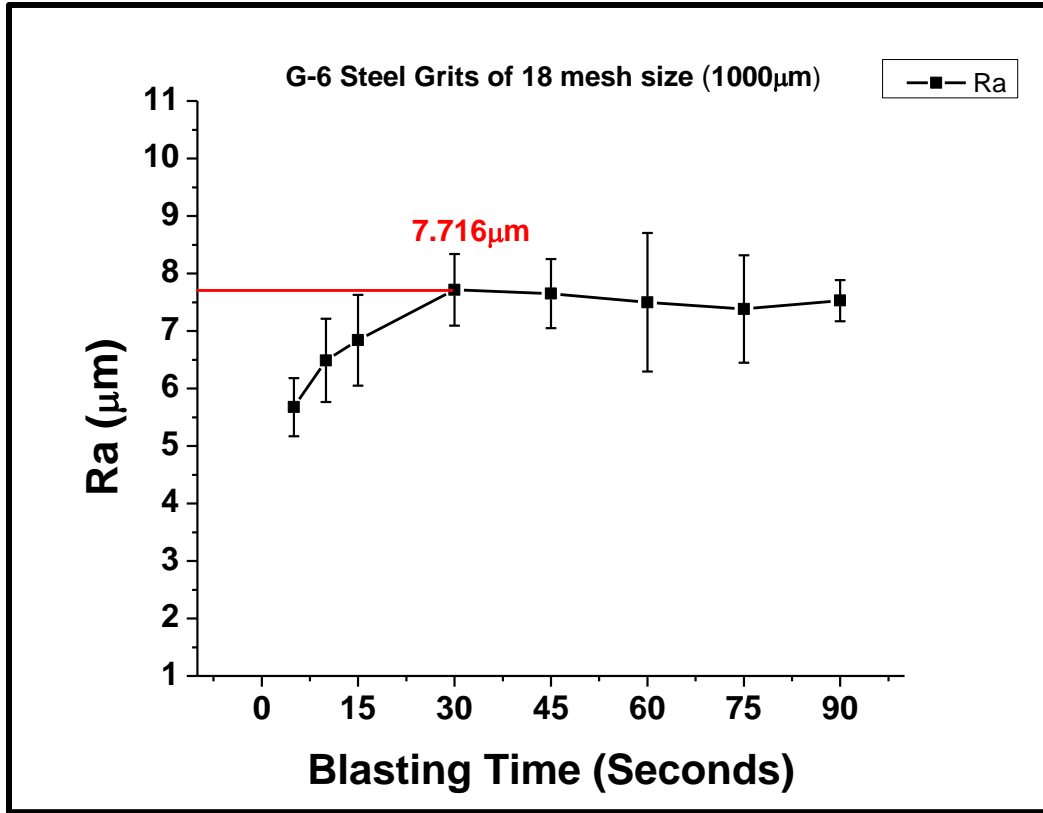
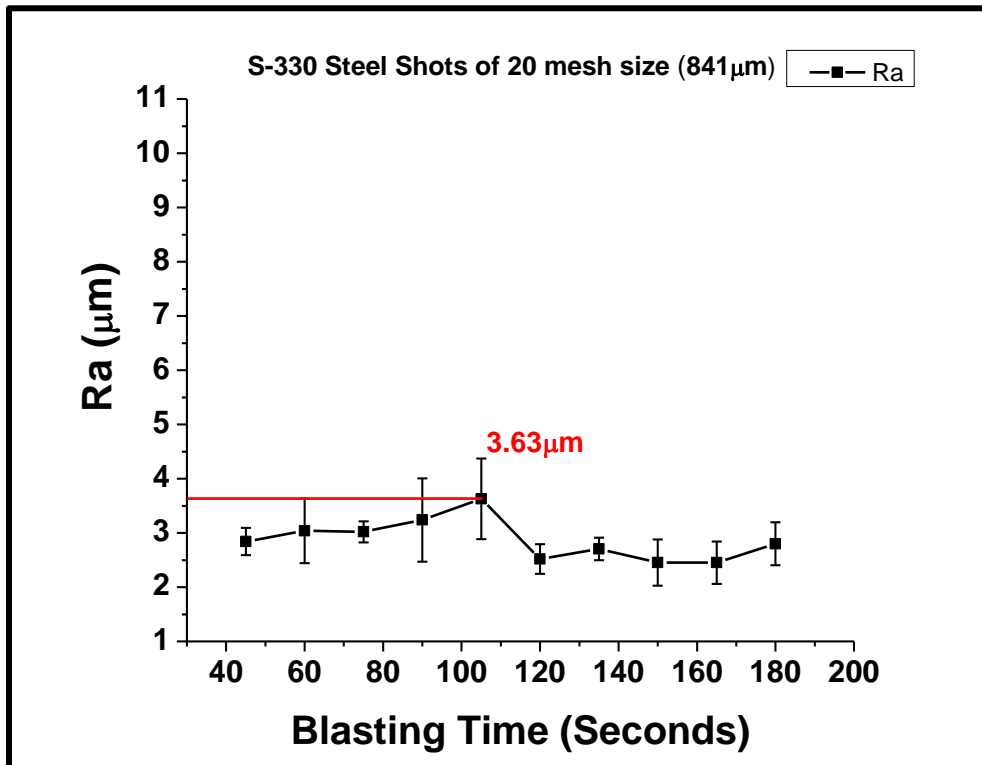


Figure 16. Ra v/s time for Alumina grits, Steel Shots and Steel Grits of 18 mesh



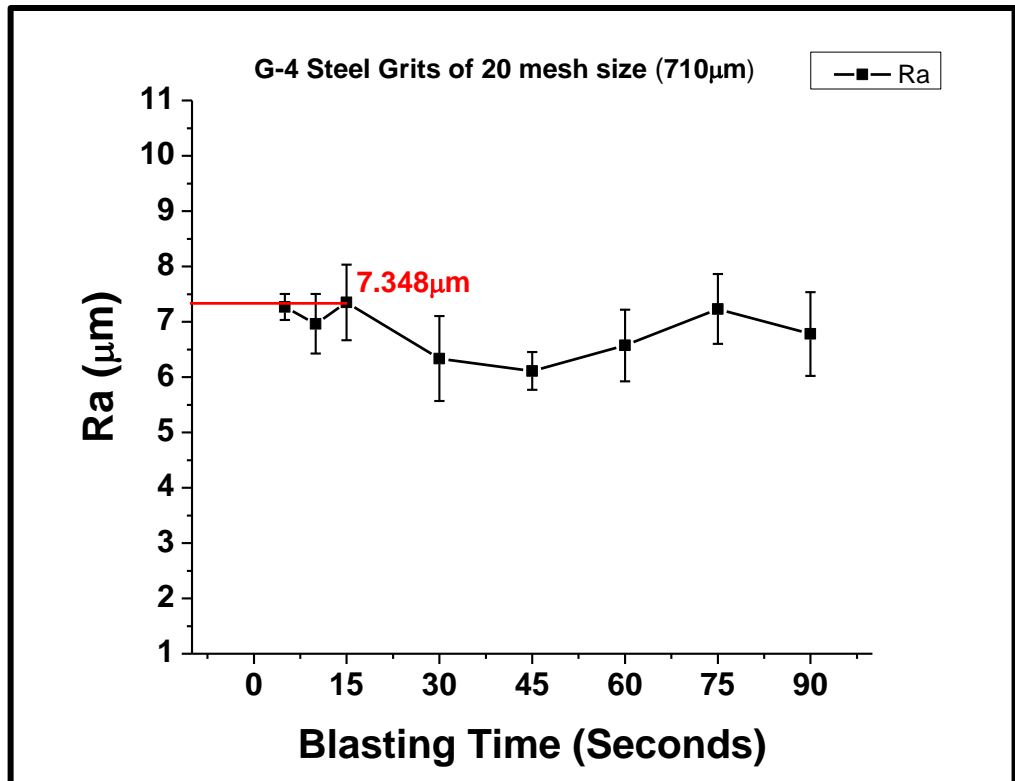
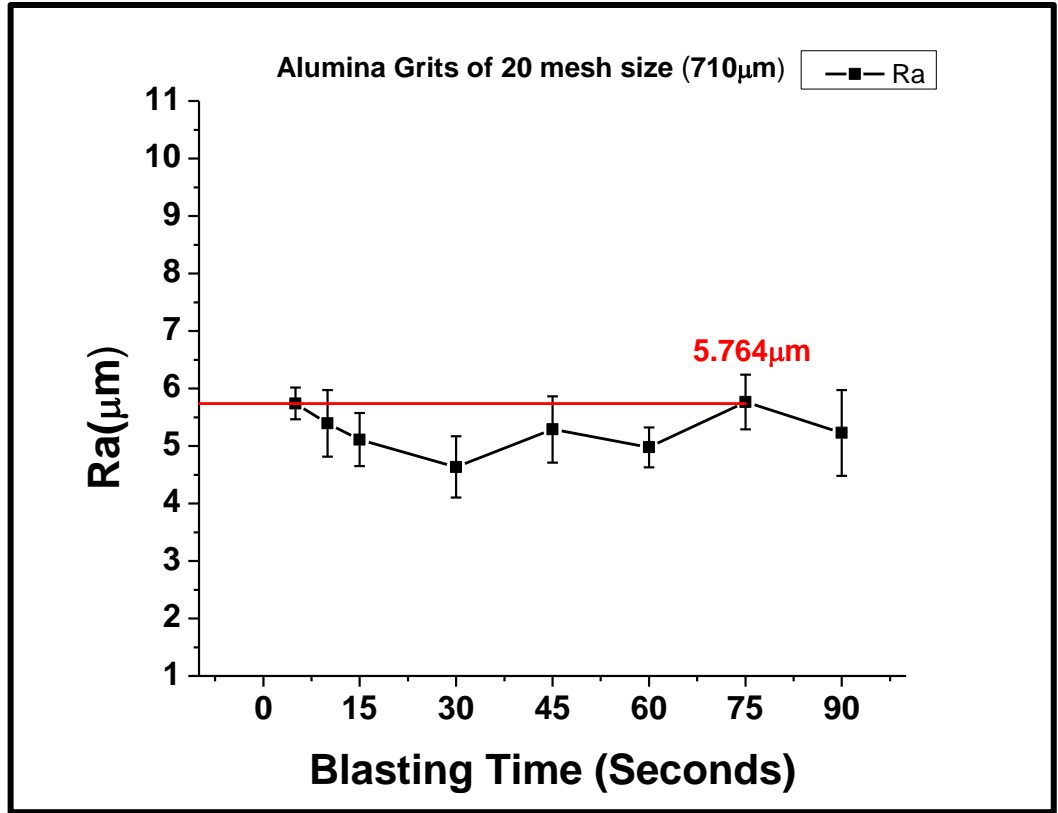


Figure 17. Ra v/s time for Alumina grits, Steel Shots and Steel Grits of 20 mesh

Owing to the highest hardness among all the Alumina grits show a very high Ra value which is achieved in a quick period. Also, the irregularities of such grit have helped it to penetrate deep into the steel surface. Similar observation is made in the case of steel grits. Apart from the deformation the machining of surface also occurs in case of irregular grits.

On the other hand, steel shots with spherical shapes are not able to penetrate or machine the surface much. The mode of roughening in this case is mostly deformation which causes development of residual stresses under the subsurface zone. Hence, blasting with steel shots for longer period time is detrimental for the life of the surface and the coating applied on it.

Although, the alumina grit has shown the best performance in terms of cleaning and roughening the surface, it has some adverse effects on the steel surface and the wheel blast blades due to its high hardness and penetration abilities. If it is used in wheel blast system, it may cause erosion to the wheel blade. In addition to this, the high embedment of such grit to the prepared steel surface may reduce the coating-substrate adhesion significantly

Another interesting observation made is, unlike spherical shots in the case of grits with increasing size the blasting time to reach the maximum Ra is increased. This is due to the limitation in achieving high indentation depth with larger grits. Among the three-blasting media used the irregular steel grits are mostly preferred due to its high cleaning ability and low negative effects on the wheel blast blade and the prepared surface.

3.3 Comparison of various blasting media w.r.t. blasting time

The blasting time to reach the maximum Ra and the reduction in blasting time with respect to the blasting media are presented in table 5.

Table 5. Comparison of different blasting media w.r.t. blasting time

Size (mesh)	Blasting Media	Time for max. Ra (s)	Blasting Time Reduction (%)
20	Steel shot (S-330)	105 s	Default
	Alumina Grit	15 s	95.2%
	Steel Grit (G-4)	18 s	85.7%
18	Steel shot (S-390)	90 s	14.3%
	Alumina Grit	5 s	95.2%
	Steel Grit (G-6)	30 s	71.4%
16	Steel shot (S-460)	60 s	42.8%
	Alumina Grit	30 s	71.4%
	Steel Grit (G-7)	60 s	42.8%

A significant reduction in blasting time is observed while using grits as blasting media for the blasting operation. The reason being material removal is caused with the help of plastic deformation in the case of shots (i.e. spherical shape of media), whereas material removal is caused with the help of micro-cutting and indentation in the case of grits (i.e. irregular shape of media). However, with larger grits the micro-cutting action is restricted by increasing the deformation effects.

3.4 Overall comparison of the blasting media

The overall comparison between the blasting media is mentioned in table 6.

Table 6. Overall comparison of blasting media

Blasting Media	Cost (Rs/kg)	Life (No. of Cycles/Impacts)	Embedment on surface	Erosion on Rotor Blade	Remarks
Steel Shots	Rs. 72/kg	High	Nil	Minimum	Good for automotive components. Material deformation is predominant over material removal. Longer blasting time. With higher size, time can be reduced.
Steel Grits	Rs. 72/kg	High	Negligible	Minimum	Excellent for industrial components. Material removal is higher than shots. Relatively faster blasting process. Often it is mixed with shots for better and quicker results.
Alumina Grits	Rs. 45/kg	Low	Relatively high	Relatively More	The fastest and most efficient blasting media. Mostly for SA 3 surface. May have some adverse effects on the produced steel surface and blast vanes/blades.

3.5 Outcomes from the experiments at CNH Pithampur

The results of the experiments performed at CNH are summarized in Table 7. It is noticed that with any selected blasting time the desired surface quality is achieved for both the side surfaces of any component. This is due to the design of the blasting chamber and the location of the rotors which are facing mainly towards the side surfaces. It is also noticed that the top, bottom, front, and rear surfaces are critical as the blasting time gets reduced. This is because of the unreachability of the shots to these surfaces due to the design constraint of the blasting chamber.

The maximum Ra on the side surfaces (LH & RH) can be obtained when the blasting time is kept around 3.30 min. However, due to the lower number of impacts on the other four surfaces (T, B, F & R) such blasting time is not sufficient for the whole component. As a result, higher blasting time (6-7 min) is required. Apart from reduced productivity, the higher blasting time causes surface hardening issues to the side surfaces by over-blasting effects. Also, the final roughness (Ra) gained on the surfaces is not very high and in the range of 5-6 μm . Clearly, higher roughness (Ra) provides increased cleaning effects. Ra value at or above 5 μm is found to show the desired surface quality of SA 2.5 or above which is suitable for subsequent coating application. This also suggests that the average thickness of oxide/rust layer on the steel (IS 2062) surface is around 5 μm . However, depending on the manufacturing process and weather condition it may increase further. For increased surface contamination blasting to create 5-6 μm Ra may not be sufficient to get the SA 2.5 surface.

In such cases, the blasting time must be increased again and increasing blasting time is not good for the life and coating of side surfaces as mentioned above. Therefore, it is recommended to keep the blasting time close to 3.30 min when the maximum Ra on the side surfaces is achieved and focus must be given on how to increase the blasting effects on the other four surfaces.

Table 7. Variation of Ra with varying blasting time for different surfaces of a component prepared by the Wheel Blast System of Paint Shop 2, CNH Pithampur

Sample	7 min (Current)		5:24 min		4:24 min		3:29 min		3:05 min	
	SA 2.5	Ra (μm)	SA 2.5	Ra (μm)	SA 2.5	Ra (μm)	SA 2.5	Ra (μm)	SA 2.5	Ra (μm)
F	Yes	6.684	Yes	5.396	No	3.4872	No	3.608	No	3.4016
R	Yes	5.0224	No	4.9288	Yes	5.6192	No	3.96	Yes	6.0552
T	No	4.3616	No	4.2832	No	3.8568	No	3.864	No	3.8488
B	Yes	5.4632	No	4.8336	No	4.5504	No	4.1952	No	4.1664
LH	Yes	6.8616	Yes	6.4944	Yes	6.7336	Yes	7.2088	Yes	6.2992
RH	Yes	5.3864	Yes	6.9232	Yes	6.9456	Yes	6.7104	Yes	6.3344

*(F-Front, R-Rear, T-Top, B-Bottom, LH-Left-hand Side, RH-Right-hand Side)

3.6 Results of the residual stress analysis

3.6.1 Residual stress analysis of the sample blasted at CNH (Airless

centrifugal blasting facility)

The residual stress analysis is carried out using XRD with the help of phi-psi (Φ - Ψ) method. Initially a phase scan is carried out for the blasted sample (with current blasting conditions at CNH Pithampur) from 2θ angle 30° to 130° . The result of the phase scan was analyzed carefully and finally the peak which appeared around 2θ angle 82° (211 peak) was selected for residual stress analysis further in the experimental work.

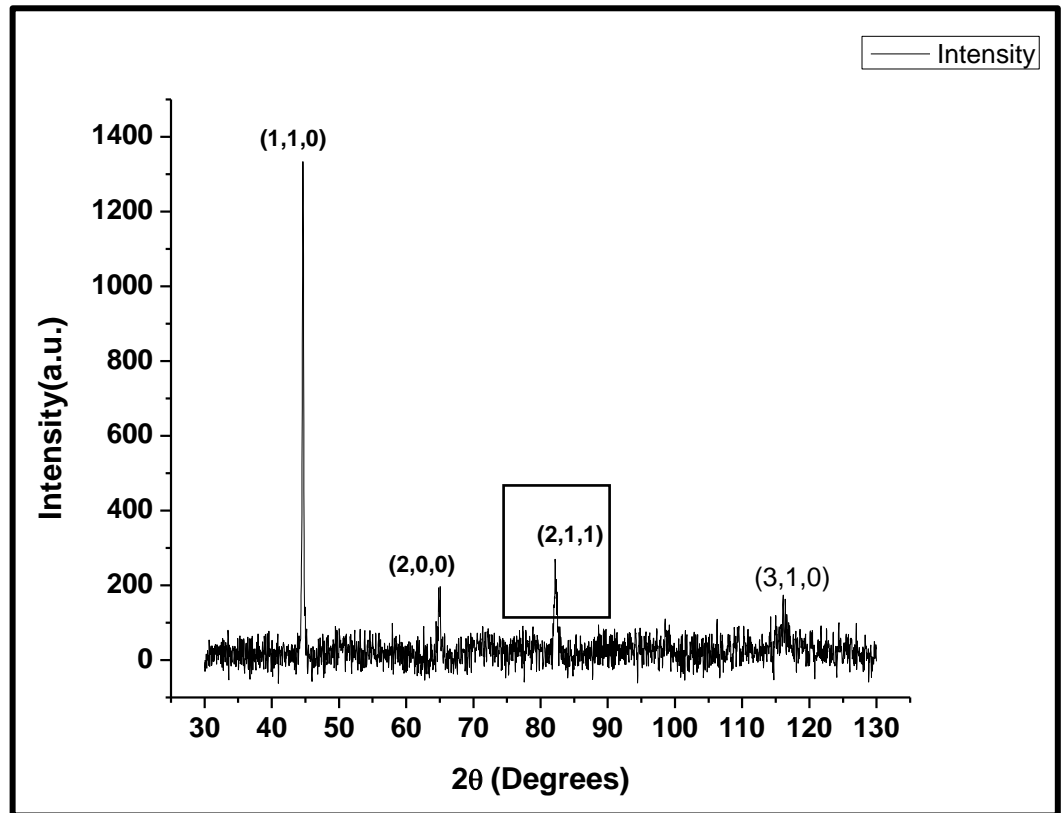


Figure 18. Normal XRD scan of the blasted sample at CNH Pithampur

Further the scans were conducted from range 80° to 84° with the step size of 0.04° . These scans are performed with different combinations of phi-psi (Φ - Ψ) angles. The combinations of phi-psi (Φ - Ψ) angles used are as follows: $\Phi = 0^\circ$ for each case and $\Psi = 0^\circ$, $\Psi = 11.537^\circ$, $\Psi = 16.43^\circ$, $\Psi = 20.268^\circ$, $\Psi = 23.578^\circ$, $\Psi = 26.565^\circ$.

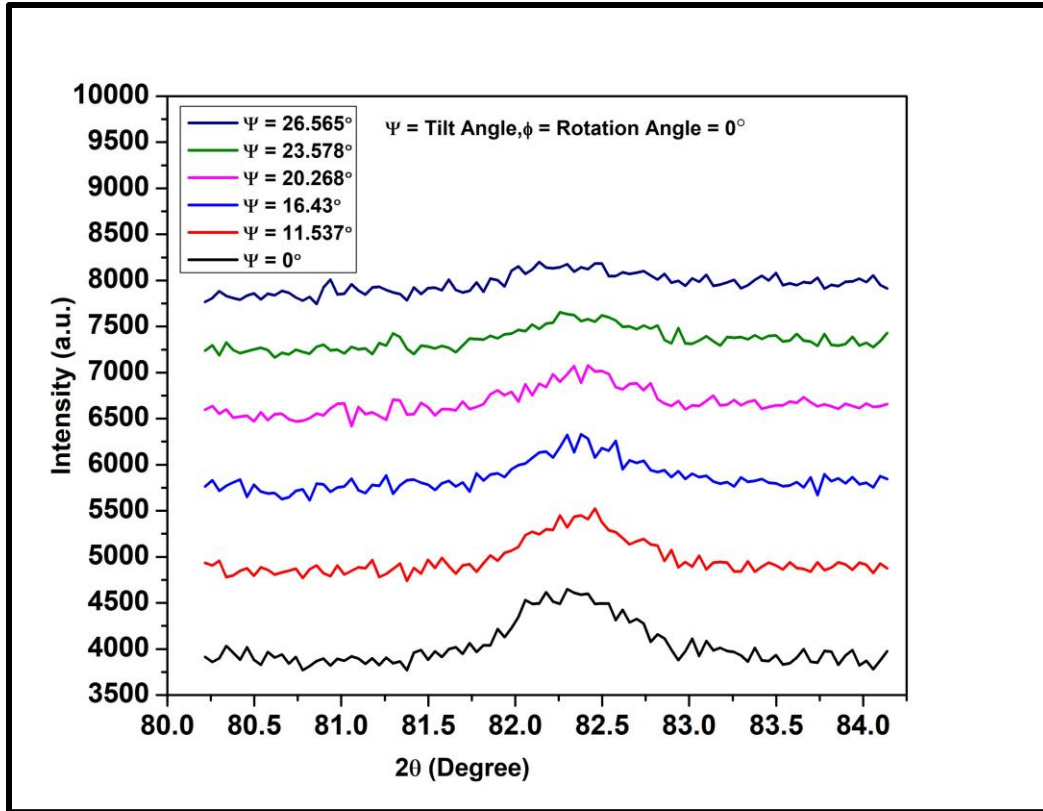


Figure 19. Residual stress analysis of the sample blasted at CNH Pithampur

It can be studied from the above figure that as the Ψ (i.e. tilt angle) increases, the significant peak observed starts to get flattened. By analyzing the individual peaks for different Ψ angles, the peak position is calculated for the respective conditions. Gaussian fit is done on each peak (for both un-blasted and blasted sample). with the help of OriginPro software, to calculate the peak position (2θ angle) of each peak. Here, in figure 20, the gauss fit to calculate the peak position for un-blasted sample is shown as an illustration. The peak position for other peaks related to different Ψ angles are calculated in the similar manner.

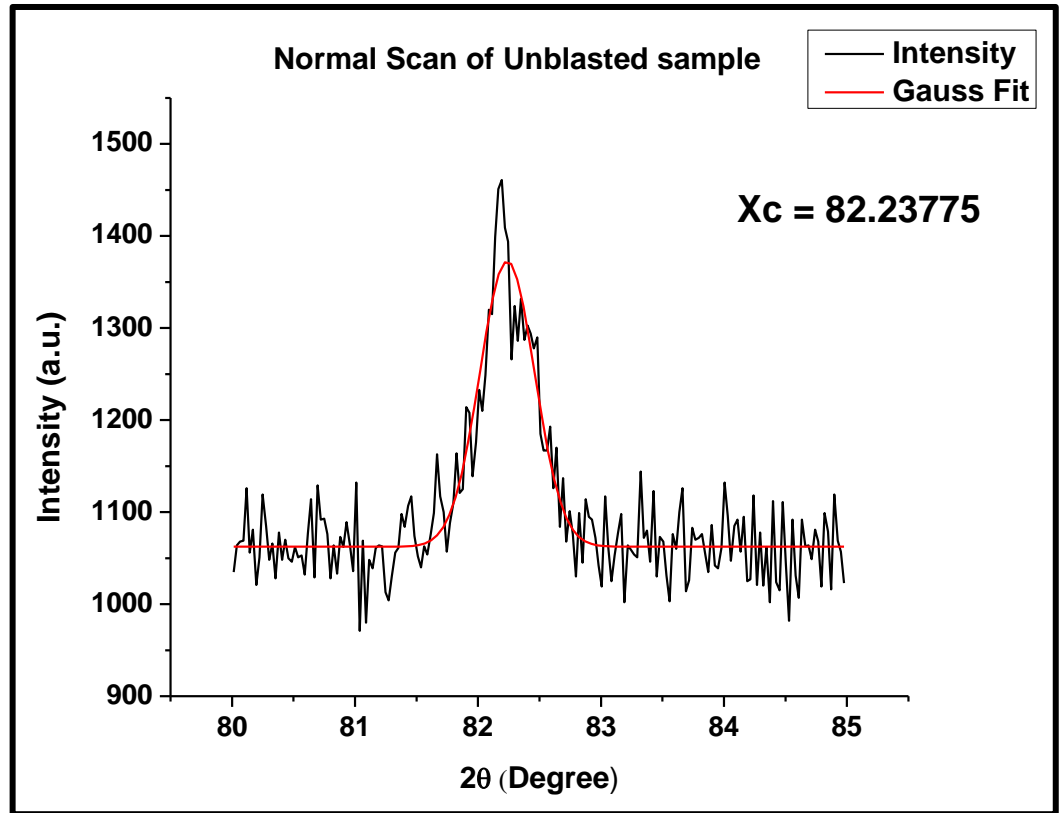


Figure 20. Gauss fit to calculate the peak position of XRD analysis for unblasted sample

The d-spacing is calculated using the peak position with the help of Bragg's law. Bragg's law can be expressed as:

$$n\lambda = 2(dn)\sin(\theta) [17]$$

Where: n is an integer representing the order of the reflection,

λ is the wavelength of the incident radiation,

d is the space between crystal planes, θ is the angle of incidence.

The following results are obtained after calculating the peak positions related to both un-blasted and blasted sample at CNH:

Table 8.d-spacing using Bragg's Law for blasted sample at CNH

Tilt Angle(Ψ) (Degrees)	Peak Position obtained from Gauss fit (2θ) (Degrees)	d_n-spacing(\AA)
0	82.33299	1.170806
11.537	82.38088	1.170247
16.43	82.38683	1.170177
20.268	82.39453	1.170087
23.578	82.41084	1.169897

Table 9.d-spacing using Bragg's Law for un-blasted sample

Peak Position (2θ) obtained from Gauss fit (Degrees)	d_0-spacing(\AA)
82.23775	1.171919892

For un-blasted sample, the d-spacing is denoted by d_0 and for the blasted sample it is denoted by d_n .

After calculating the values of d-spacing in both blasted and un-blasted samples, the strain is calculated using the formula $(d_n - d_0)/d_0$. This is the strain obtained in the laboratory conditions, i.e. the strain obtained in the different combinations of phi-psi (Φ - Ψ) angles. **These values are expressed as ϵ_{33}** . The values obtained are listed in the table below:

Table 10. Calculation of laboratory strain values for the sample blasted at CNH

Tilt Angle(Ψ) (Degrees)	d_n (Å)	d_0 (Å) (w.r.t. un-blasted sample)	Strain ϵ_{33}' ($(d_n - d_0)/d_0$)
0	1.170806	1.171919892	-0.0009507
11.537	1.170247		-0.0014278
16.43	1.170177		-0.001487
20.268	1.170087		-0.0015636
23.578	1.169897		-0.0017259

These results of the laboratory strain values are useful to calculate the actual strain values in all the directions in the blasted sample. A schematic diagram of the directions of stresses induced when the load (either tensile or compressive) is applied on a specimen, can be shown as follows:

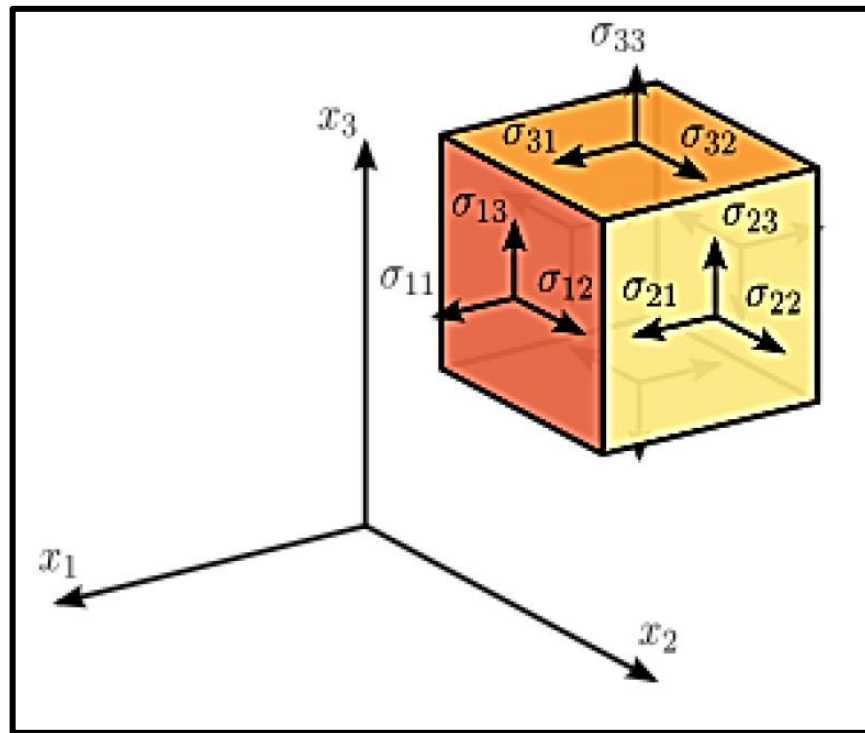


Figure 21. Schematic diagram of the types and directions of stresses induced due to application of load on a specimen

Here, σ_{12} , σ_{13} , σ_{23} are out of plane and σ_{11} , σ_{22} , σ_{33} are in-plane stresses. ϵ_{12} , ϵ_{13} , ϵ_{23} , ϵ_{11} , ϵ_{22} , ϵ_{33} are the respective values of strain associated. It is to be noted that the **blasting was carried out along the direction X3**. Thus, it is expected that **compressive residual stress** will be obtained **along the direction X3** because of the further analysis and calculations.

The relationship between the laboratory strain values and the actual strain values can be given by the following equation[18]:

$$\begin{aligned} \epsilon'_{33} = & \epsilon_{11} \cos^2 \phi \sin^2 \psi + \epsilon_{12} \sin 2\phi \sin^2 \psi + \epsilon_{22} \sin^2 \phi \sin^2 \psi \\ & + \epsilon_{33} \cos^2 \psi + \epsilon_{13} \cos \phi \sin 2\psi + \epsilon_{23} \sin \phi \sin 2\psi \end{aligned}$$

Here, we can obtain a system of linear equations by substitution of values for each combination of Φ - Ψ angles that have been incorporated for the XRD analysis of the blasted sample. Calculating the unknown coefficients by solving the system of equations (by substituting values: ϵ'_{33} , Ψ , and $\Phi = 0$) we get:

$$\epsilon_{11} = \mathbf{-0.0003}$$

$\epsilon_{22} = \mathbf{-0.0003}$ (Here its assumed that $\epsilon_{22} = \epsilon_{11}$ because of axis symmetric deformation).

$$\epsilon_{33} = \mathbf{-0.001}$$

$$\epsilon_{13} = \mathbf{-0.0011}$$

These are the values of strain in the normal conditions in the different in plane and out of plane directions in the sample. The strain values in the samples can be useful to calculate the residual stress.

The relationship between the strain induced in the material on the application of load, and the corresponding residual stress can be defined as follows[19]:

$$\begin{bmatrix} \sigma_{11} \\ \sigma_{22} \\ \sigma_{33} \\ \sigma_{23} \\ \sigma_{31} \\ \sigma_{12} \end{bmatrix} = \frac{E}{(1+\nu)(1-2\nu)} \begin{bmatrix} 1-\nu & \nu & \nu & 0 & 0 & 0 \\ \nu & 1-\nu & \nu & 0 & 0 & 0 \\ \nu & \nu & 1-\nu & 0 & 0 & 0 \\ 0 & 0 & 0 & (1-2\nu)/2 & 0 & 0 \\ 0 & 0 & 0 & 0 & (1-2\nu)/2 & 0 \\ 0 & 0 & 0 & 0 & 0 & (1-2\nu)/2 \end{bmatrix} \begin{bmatrix} \varepsilon_{11} \\ \varepsilon_{22} \\ \varepsilon_{33} \\ 2\varepsilon_{23} \\ 2\varepsilon_{31} \\ 2\varepsilon_{12} \end{bmatrix}$$

Here E denotes the Young's modulus of steel, which is equal to 200 GPa, and ν denotes the Poisson's ratio of steel which is equal to 0.28. The system of linear equations can be obtained by substituting the values of the strain in normal condition in the above equation. Solving for σ_{11} , σ_{33} , σ_{13} we get:

$$\sigma_{11} = -205.966 \text{ MPa}$$

$$\sigma_{33} = -315.341 \text{ MPa}$$

$$\sigma_{13} = -140.8 \text{ MPa}$$

The above results indicate that a significant amount of compressive residual stress is present in the sample blasted at the blasting facility of CNH Pithampur. Out of the values obtained, the σ_{33} value is the value of concern for the study, as the blasting is done along the direction X3 as per the indication in figure 21.

3.6.2 Residual Stress analysis of the samples blasted at Suction type blasting facility(IIT Indore)

The residual stress analysis is done for the samples blasted at Suction type blasting facility, IIT Indore using the blasting media like steel grits, steel shots and alumina grits. Two mesh sizes for all the blasting media namely 16 Mesh size and 20 Mesh size are selected to prepare the samples by blasting. The procedure to calculate the residual stress is same as mentioned in the section 3.6.1. Initially, the XRD scan of the individual samples is done with the respective Φ - Ψ combination of $\Phi = 0^\circ$, $\Phi = 90^\circ$ and $\Psi = 0^\circ$, $\Psi = 11.537^\circ$, $\Psi = 16.43^\circ$, $\Psi = 20.268^\circ$, $\Psi = 23.578^\circ$, $\Psi = 26.565^\circ$.

The results of these scans were analyzed and finally the laboratory strain value ε_{33} ' was calculated by following the similar approach as discussed

earlier for the sample blasted at CNH. The resultant values of ϵ_{33} were useful in calculating the actual strain values, which were finally used to calculate the residual stress for all the blasted samples. The figure shows the results of the residual stress of the blasted samples at the suction blasting facility:

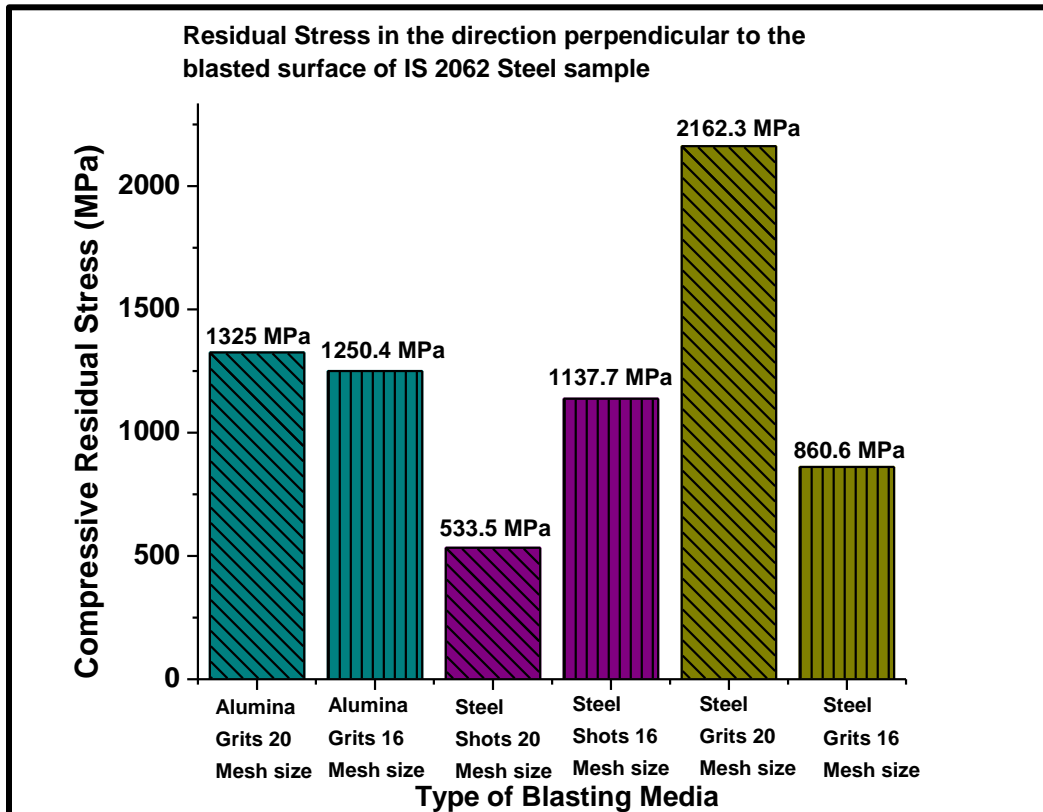


Figure 22. Comparison of residual stress among the samples blasted with different blasting media and mesh sizes

It is to be noted that in the above comparison, the values σ_{33} are mentioned because, that indicates the value of the residual stress generated perpendicular to the blasted surface.

3.7 Observations from the Vickers Microhardness analysis of the cross section of the blasted samples

The Vickers microhardness analysis of the cross section of blasted samples shows that the value of hardness shows a decreasing trend as the analysis is done from top to the base of the cross section. After a certain distance, the

hardness of the cross section becomes uniform. This value of the distance shows the depth of the residual stress that is induced due to the blasting operation on the IS-2062 steel samples. The depth of hardened zone in this study is calculated by linear extrapolation of the best-fit-line of the plot of microhardness values, against the depth of cross section of the blasted sample. The graphs of the microhardness analysis are mentioned in Figures 23, 24 and 25.

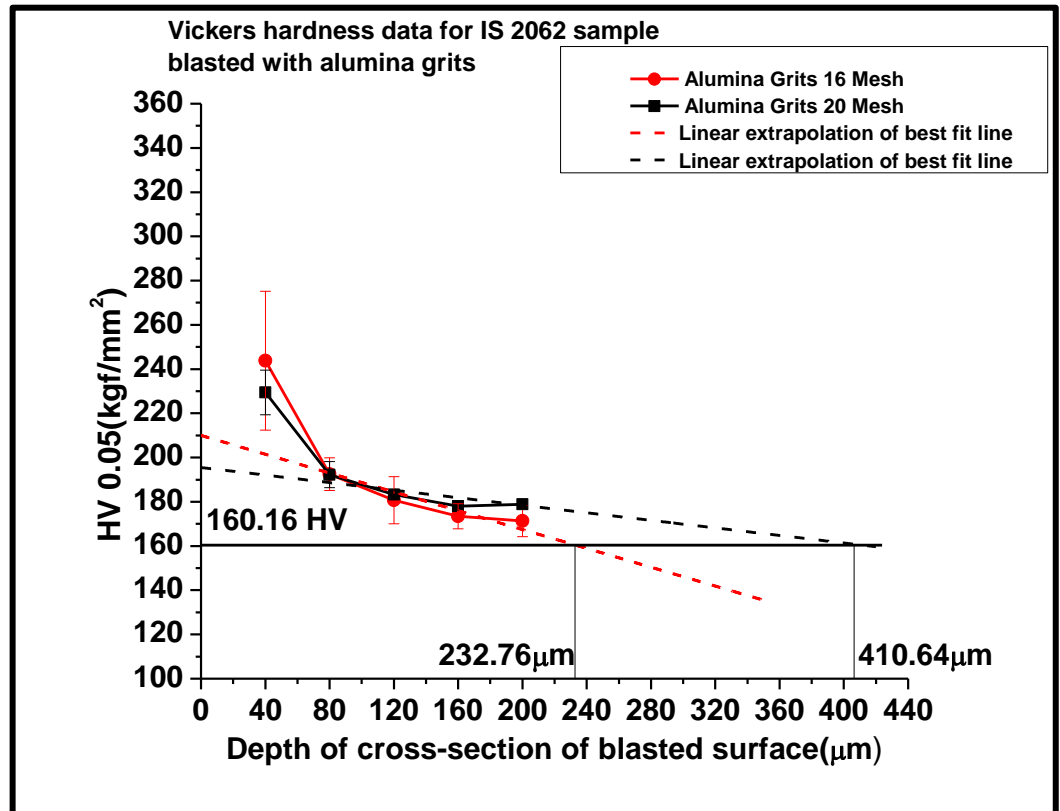


Figure 23. Vickers microhardness data plot for Alumina grits 16 mesh size and 20 mesh size

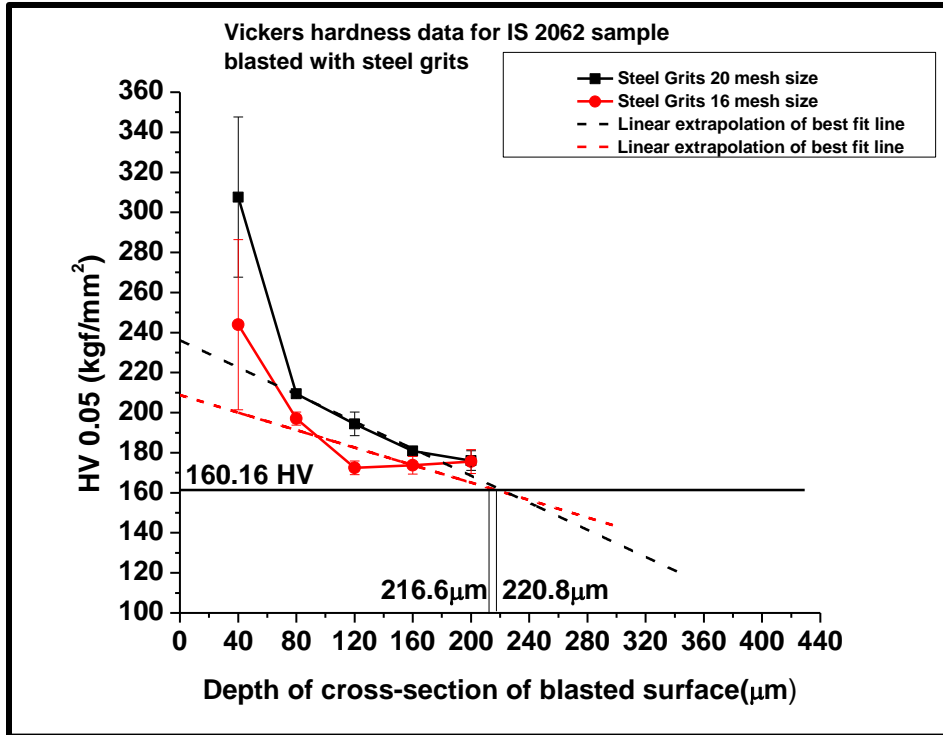


Figure 24. Vickers microhardness data plot for Steel grits 16 mesh size and 20 mesh size.

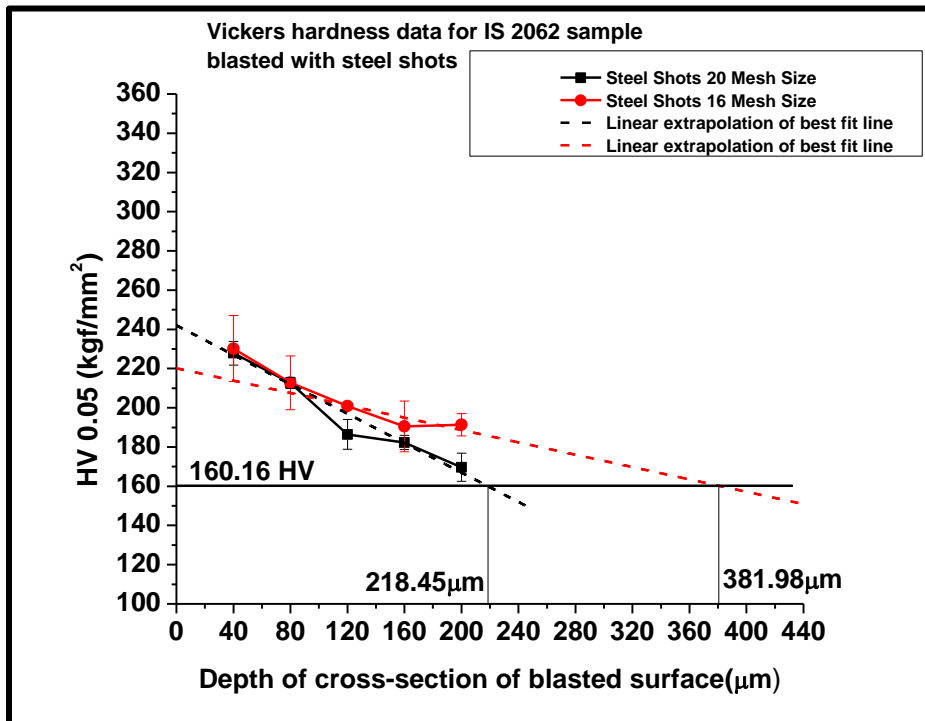


Figure 25. Vickers microhardness data plot for Steel shots 16 mesh size and 20 mesh size

The following table shows the comparison of the depth of hardened zone, hardness and residual stress in samples blasted with different blasting media and Mesh size.

Table 11. Comparison of depth of residual stress generated on IS-2062 when blasted with different blasting media and size

Blasting Media	Size (Mesh)	Residual Stress (MPa)	HV _{0.05} (kgf/mm ²) (at top)	Depth of hardened Zone (μm)
Alumina Grits	20	1325	230	410.64
	16	1250.4	245	232.76
Steel Grits	20	2162.3	310	220.8
	16	860.6	245	216.6
Steel Shots	20	533.5	230	218.45
	16	1137.7	230	381.98

3.8 Weight measurement of IS-2062 steel samples and different blasting media

3.8.1 Weight measurement of IS-2062 steel samples

A comparative study related to weight measurement is carried out for rusted IS-2062 samples by blasting the samples with alumina grits, steel grits and steel shots with the mesh sizes of 16, 18 and 20 mesh respectively. The blasting is performed from 30 seconds to 90 seconds with an increment of 15 seconds of blasting time after each operation. The weight of the sample is recorded with a weighing scale after each operation. The weight loss after each stage of blasting operation is calculated with respect to the original weight of the sample before blasting. The graphs of the weight loss of IS-2062 related to each type of blasting media are shown in Figures 26 to 28.

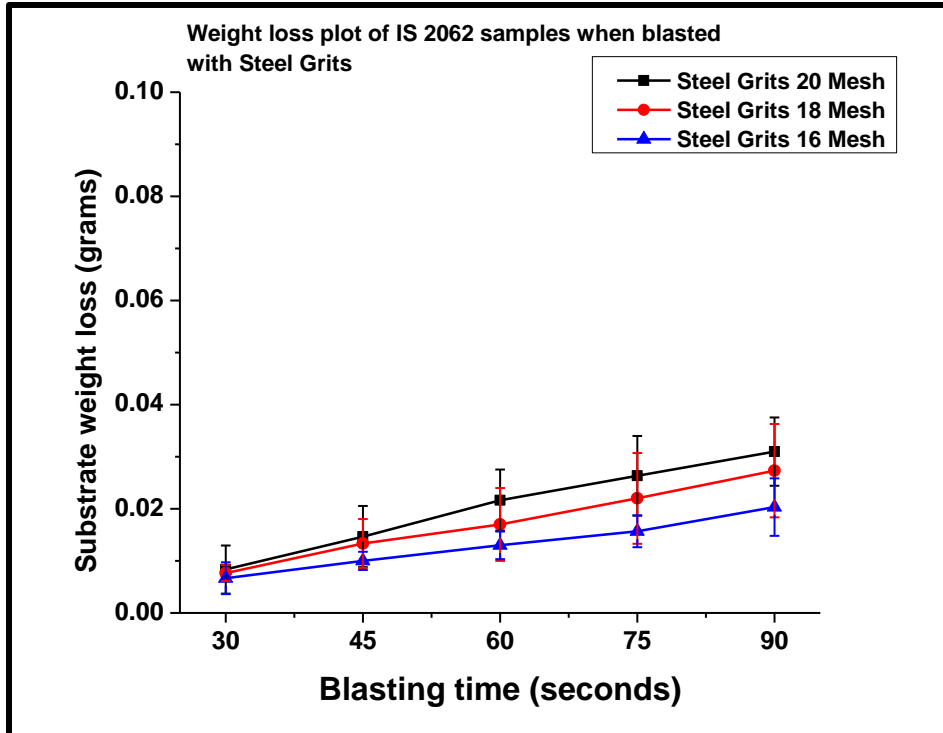


Figure 26. Weight Loss of IS-2062 samples when blasted with steel grits

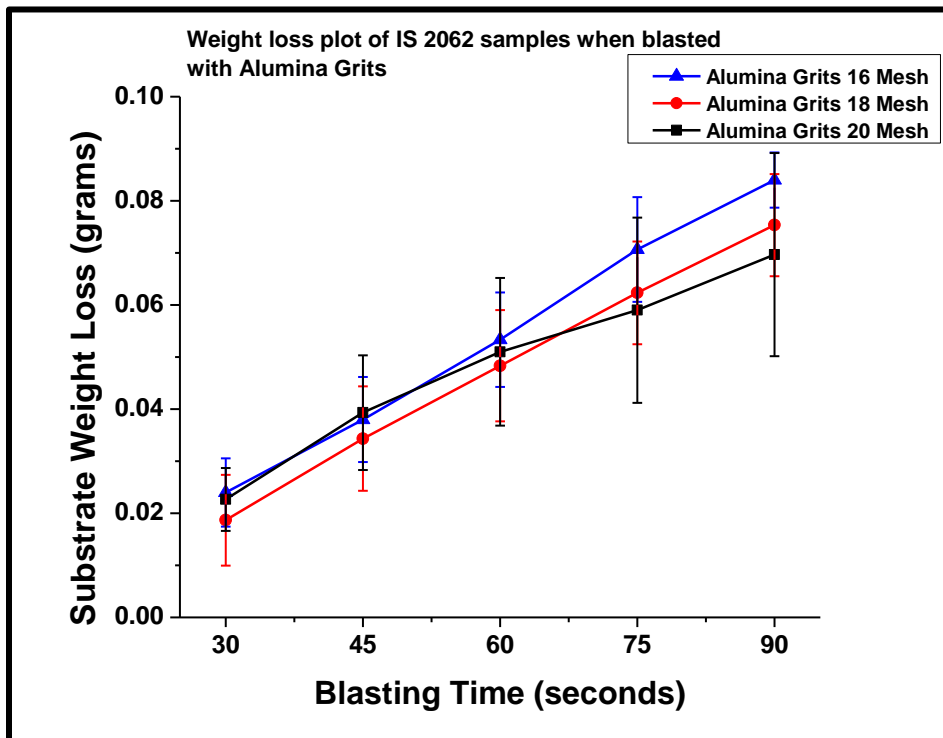


Figure 27. Weight loss of IS-2062 samples when blasted with Alumina grits

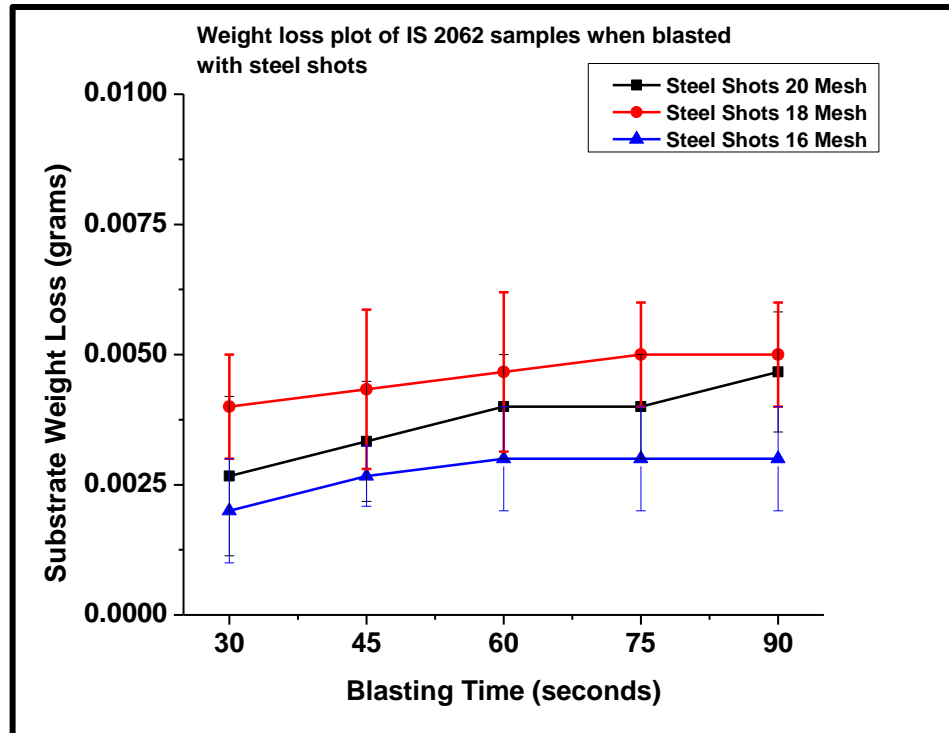


Figure 28. Weight loss of IS-2062 samples when blasted with Steel shots

It can be studied from the above graphs that the highest weight loss of sample takes place when blasted with alumina grits, followed by steel grits. In the case of blasting with steel shots, the sample does not lose weight in a significant manner. This is because alumina grits are harder than steel grits and thus it removes more material due to micro-cutting than that of the steel grits. In case of comparing the shape of blasting media, the grits remove more weight than shots because in case of shots the material removal takes place through deformation unlike in the case of grits in which the mechanism of material removal is micro-cutting and indentation. The material removal in the case of steel shots is almost zero because of the deformation of the blasted surface. Comparing the size of the blasting media, the small size of the media removes the material more effectively than the larger size because smaller media has better penetration ability than the larger size media. Also, the number of impacts is more in the case of smaller blasting media because of better flow rate from the blasting nozzle than the larger size blasting media.

3.8.2 Weight measurement of blasting media

The weight measurement of blasting media is studied to check the effectiveness of the different blasting media. For this experiment, the rusted IS-2062 samples are blasted for 15 seconds, and the blasting media is changed one by one after every experiment. The samples of blasting media are collected from the hopper of the machine by ensuring only those particles of the blasting media be collected that participated in the blasting operation. Then, the weight difference is calculated for a suitable number of blasting media. The result of this analysis is shown in the figure 29 :

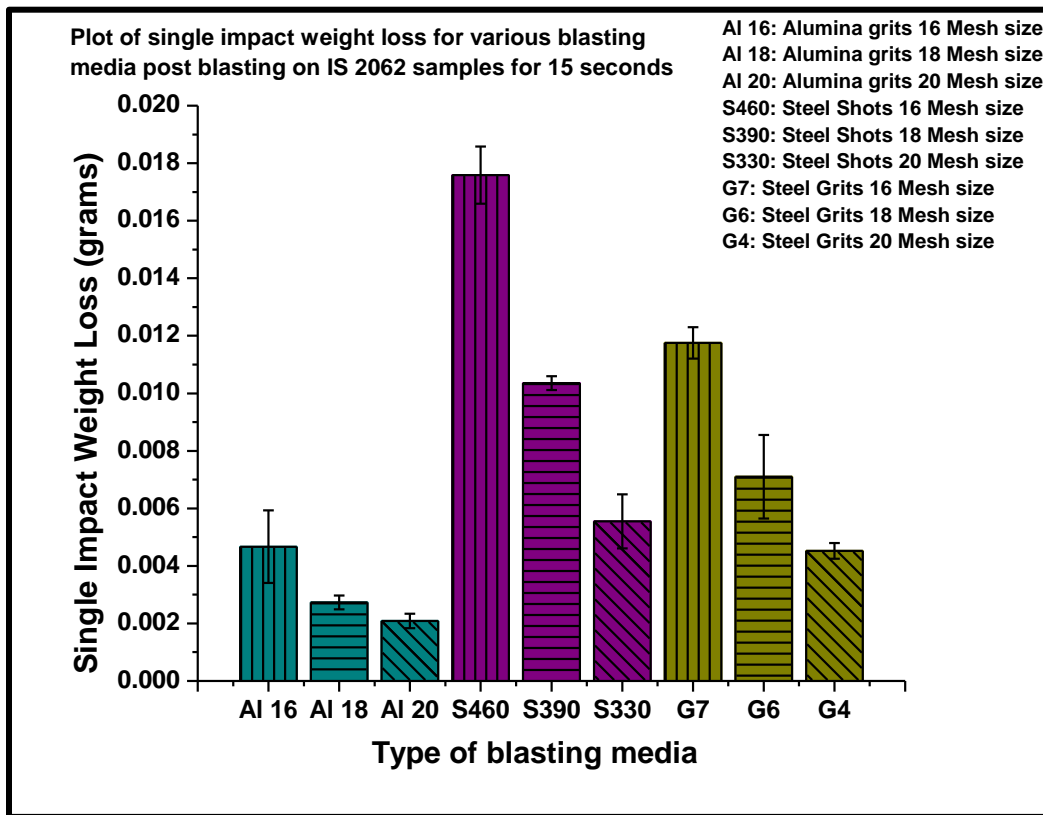


Figure 29. Comparison of Single impact weight for various blasting media

It can be observed from Figure 29 that blasting media with larger mesh size is more durable than that with the smaller mesh size, because it loses less weight compared to its smaller counterparts after equal amount of blasting on IS-2062 samples. This happens because due to the larger size, the energy impact on the blasting media due to blasting on the substrate occurs in a significant manner, thus reducing the weight. Comparing the material of

blasting media, steel shots show the highest weight loss followed by steel grits and alumina grits respectively. This happens because due to the deformation of the surface, the steel shots bounce back instead of penetrating the surface. Due to this, the steel shots lose weight in a significant manner.

CHAPTER 4: Conclusion

4.1 Suggestions for the airless centrifugal wheel blasting facility to reduce the blasting time without changing the blasting media

As per the previous discussions, it is recommended to keep the blasting time close to 3.30 min when the maximum Ra on the side surfaces is achieved and focus must be given on how to increase the blasting effects on the other four surfaces.

The following suggestions can be adopted to improve the blasting effects on these surfaces without changing the blasting media:

1. Manipulation (rotation along a vertical axis) of components in the blasting chamber during forward movement:

It will blast the front (F) and rear (R) surfaces effectively and efficiently. However, this will reduce the number of components in a single batch to provide additional space for rotation. Also, for large components it may not be possible considering the shape and size of the component.

2. Design change of the blasting chamber:

One of the rotors from each wall should aim towards the front (F) and rear (R) surfaces. Currently, angular movement of rotors is possible in vertical direction only. This can be optimized for effective blasting on the top (T) and bottom (B) surfaces. Also, the top and bottom surfaces of the component should be placed at a distance of at least 2 ft from the hanging shaft and chamber floor respectively. Reflector plates (as already placed on the floor for B surface) may be attached to the hanging shaft for increased impact on the top (T) surface. It is better to keep the component close to the middle zone of the blasting volume.

3. Increased flow rate of blasting media:

The flow rate of blasting media (shots/grits) may be increased to increase the number of impacts on the surfaces. This will reduce the blasting time further from 3:30 min to achieve the maximum Ra on the side surfaces. Also, it will enhance the number of impacts on the unreachable surfaces.

4. Switching on the rotors (blasting operation) at proper time:

Once the blasting volume (entire batch) just enters the chamber the rotors of the first chamber may start to get increased impacts on the front surface (F). Also, the rotors of the second chamber should remain on until the rear (R) surface is out of the chamber. This will enhance the number of impacts on the front and rear surfaces to some extent.

4.2 Other suggestions and conclusions related to the airless centrifugal blasting facility

- By using larger steel shots (S-390/S-460) or steel grits (G-4, G-6, G-7) the blasting time can be reduced significantly. With high penetration capability the steel grits (irregular) show better results than the steel shots. In many industries steel shots are mixed with steel grits with suitable proportion for improved performance. Thicker oxide layers and mill scales can be removed efficiently by the steel grits. The detrimental effect of steel grits on the rotor blades is also negligible. Although alumina grits show the best results, considering the negative impacts of such material on the blades, steel surface and the environment such material is not recommended.
- Currently the high blasting time required for producing desired surface is due to the unreachability of shots to the top, bottom, front and rear surfaces. At any selected time, the side surfaces show the desired results due to the increased number of impacts. The maximum Ra for such surfaces is obtained for the time of around 3:30 min.
- Without changing the blasting media, the blasting time of the Wheel Blast system of CNH can be reduced by giving rotation to the components, changing the design of the chamber (rotor position and angle), application of reflector plate at the top and switching on the blasting operation at proper time.

4.3 Overall Conclusions

- Larger steel shots can produce the desired surface quicker than the smaller shots. A higher mass of the shots helps to improve the kinetic energy of the media.
- Grits can produce the desired surface quicker than the shots. Also, Grits can provide higher Ra than the same from shots. Smaller grits are more effective than larger grits due to their higher penetration ability.
- With an increase in time, the weight of the substrate does not change much in case of steel shot due to its deformation effect. However, in the case of grits the weight of the substrate reduces significantly and almost linearly due to the machining effect. Among the two different grit materials, alumina grits can remove material faster than steel grits. This is due to the high hardness and disintegration property of the alumina grits.
- The life of smaller grit/shot is more than the larger one. Due to the high impact energy larger grit/shot disintegrate faster than the smaller one. Among different blasting media steel shot shows the minimum life with lowest disintegration property, whereas the alumina grit shows the maximum life with the highest disintegration property.
- The residual stress of shot/grit blasted steel surfaces is compressive in nature. In general, this stress is more in case of blasting by grits than by the shots. High compressive stress results in high hardness which is mostly confined to the top surface (up to 80 μm depth). The reduction in hardness with increasing depth is more regular and linear in the case of steel shots. Among all, the highest residual stress is obtained when blasted with steel grits of 20 mesh size. However, residual stress can be influenced by other parameters too.

4.4 Future Scope of Work

- Surface roughness study and residual stress measurement can be carried out for substrates blasted by mixing different blasting media in suitable proportions.
- The effect of surface quality produced by different blasting media on the adhesion of coatings can be studied.

REFERENCES

- [1] Fundamental of surface engineering- NPTEL, Dr. D.K. Dwivedi

- [2] Kim et.al (2021), Surface Characteristics and Corrosion Behavior of Carbon Steel Treated by Abrasive Blasting. (DOI: 10.3390/met11122065)
- [3] Pradhan, G.K. (1996). Explosives and Blasting Techniques. Mintech Publications.
- [4] Whelan, T. (2008). Media selection for micro blasting medical parts. *Medical Device Technology*, 19(6), 36, 38-40.
- [5] <https://www.kramerindustriesonline.com/product/aluminum-oxide-grit/>
- [6] <https://www.kramerindustriesonline.com/product/glass-beads/>
- [7] <https://m.indiamart.com/proddetail/steel-shot-s330-22425942548.html>
- [8] <https://www.casece.com/en/asiapacific/case-world/inside-case/our-plants>
- [9] Bahbou et al. (2004), Effect of grit blasting and spraying angle on the adhesion strength of a plasma-sprayed coating. (DOI: 10.1361/10599630421406)
- [10] James Day et al. (2005), Examination of a grit-blasting process for thermal spraying using statistical methods (DOI: 10.1361/105996305X76469)
- [11] K Poorna Chander et al. (2009), Effects of grit blasting on surface properties of steel substrates. *Materials and Design* 30 (2009) 2895–2902 (DOI:10.1016/j.matdes.2009.01.014)
- [12] M Multigner et al. (2009), Interrogations on the sub-surface strain hardening of grit blasted Ti-6Al-4V alloy, *Surface and Coatings Technology* 203(14):2036-2040 (DOI:10.1016/j.surfcoat.2009.02.003)

- [13] Vishal Sharma and Kazi Sabiruddin (2020), A comparative study of sand-blasted and electro-discharge-machined surfaces of steel substrates, (DOI:10.1007/s12046-020-1267-x)
- [14] Prathamesh Tawade et al. (2023), Effects of different Grit Blasting Environments on the prepared steel Surface, J Therm Spray Tech (2023) 32:1535–1553 (<https://doi.org/10.1007/s11666-023-01585-3>)
- [15] M Praveen et al. (2023), Surface cleaning of IS-2062 E350 grade steel plates by using a multi table air type shot blasting machine. (<https://doi.org/10.1016/j.matpr.2023.06.139>)
- [16] Bureau of Indian Standards (BIS). (2020). IS 1501 (Part 1): 2020 Metallic Materials — Vickers Hardness Test Part 1 Test Method. (https://www.services.bis.gov.in/php/BIS_2.0/bisconnect/standard_review/Standard_review/Isdetails?ID=Mzgy)
- [17] Greenberg, B. (1989). Bragg's law with refraction. Acta Crystallographica Section A, 45, 238-241. (DOI: 10.1107/S0108767388012243).
- [18] Callister, W. D., & Rethwisch, D. G. (2018). Fundamentals of Materials Science and Engineering: An Integrated Approach (5th ed.). Wiley. ISBN: 978-1119175483.
- [19] Bonet, J., & Wood, R. D. (1997). Finite element formulations for large strain anisotropic elasticity: Continuum basis and numerical aspects. Computer Methods in Applied Mechanics and Engineering.